1.19 Venus

B. Fegley, Jr.

Washington University, St. Louis, MO, USA

1.19.1 BRIEF HISTORY OF OBSERVATIONS

1.19.1.1 Pre-twentieth Century

Venus is Earth's nearest planetary neighbor, and has fascinated mankind since the dawn of history. Venus' clouds reflect most of the sunlight shining on the planet and make it the brightest object in the sky after the Sun and Moon. Venus is visible with the naked eye as an evening star until a few hours after sunset, or as a morning star shortly before sunrise. Many ancient civilizations observed and worshipped Venus, which had a different name in each society, e.g., Ishtar to the Babylonians, Aphrodite to the Greeks, Tai'pei to the Chinese, and Venus to the Romans (Hunt and Moore, 1982). Venus has continued to play an important role in myth, literature, and science throughout history.

In the early seventeenth century, Galileo's observations of the phases of Venus showed that the geocentric (Ptolemaic) model of the solar system was wrong and that the heliocentric (Copernican) model was correct. About a century later, Edmund Halley proposed that the distance from the Earth to the Sun (which was then unknown and is defined as one astronomical unit, AU) could be measured by observing transits of Venus across the Sun. These transits

occur in pairs separated by eight years at intervals of 105.5 yr and 121.5 yr in an overall cycle of 243 yr, e.g., June 6, 1761, June 3, 1769; December 9, 1874, December 6, 1882, June 8, 2004, June 6, 2012, December 11, 2117, and December 8, 2125.

The first attempted measurements of the astronomical unit during the 1761 transit were unsuccessful. However, several observers reported a halo around Venus as it entered and exited the Sun's disk. Thomas Bergman in Uppsala and Mikhail Lomonosov in St. Petersburg, independently speculated that the halo was due to an atmosphere on Venus. Eight years later observations of the 1769 solar transit (including those made by Captain Cook's expedition to Tahiti) gave a value of 1 AU = 153 million kilometers, ~2.3% larger than the actual size (149.6 million kilometers) of the astronomical unit (Woolf, 1959; Maor, 2000).

1.19.1.2 The Twentieth Century to the Present Day

Modern observations of Venus date to the 1920s. During this decade Wright and Ross took the first UV photographs and discovered the UV dark markings in the clouds. Also in the 1920s, Pettit and Nicholson measured Venus' temperature as 240 K. Venus' atmospheric composition remained unknown until 1932, when Adams and Dunham serendipitously discovered CO_2 during an unsuccessful spectroscopic search for water vapor. Subsequent laboratory spectroscopy by Adel and Slipher in 1934 showed that Venus' atmosphere contains much more CO_2 than Earth's atmosphere. Shortly thereafter, in 1940, Wildt proposed that the large amount of CO_2 in Venus' atmosphere caused greenhouse heating and concluded that Venus' surface temperature "appears to be higher than the terrestrial boiling point of water." Wildt's idea, which was explored in more detail by Sagan in the early 1960s, was verified by microwave observations from Earth in the late 1950s and from Mariner 2 during its historic 1962 flyby (Barath *et al.*, 1964).

From the late 1950s onward, Venus has been subjected to a variety of increasingly sophisticated Earth-based, Earth-orbital, and spacecraft observations. Spectroscopic observations of Venus were carried out using high-altitude telescopes carried on balloons or on airplanes. Fourier transform infrared (FTIR) spectrometers were applied to planetary spectroscopy and were used to observe Venus. As a result, the $^{13}C/^{12}C$ and $^{18}O/^{16}O$ isotopic ratios in CO_2 on Venus were measured and H_2O, CO, HCl, and HF were discovered in Venus' atmosphere (Connes *et al.*, 1967, 1968; Bézard *et al.*, 1987). During the 1960s, Earth-based radar observations measured Venus' radius, rotation rate, pole position, proved that Venus rotates in a retrograde (i.e., east to west) direction, and gave the first radar "images" of its surface, which cannot be seen through the thick atmosphere and clouds (Pettengill, 1968; Shapiro, 1968).

In the early 1970s, Earth-based measurements of the polarization and refractive index of the cloud particles led to their identification as droplets of concentrated (~75% by mass) sulfuric acid (Esposito *et al.*, 1983). Several years later, Barker (1979) discovered SO_2 at Venus' cloud tops. Almost simultaneously, instruments on the *Pioneer Venus* and *Venera 11–12* missions also observed SO_2.

The *Pioneer Venus* mission provided the first radar imaging and altimetry of Venus' surface from synthetic aperture radar on an orbiting spacecraft. Subsequently, the *Venera 15* and *16* orbiters also carried out radar imaging and altimetry of part of Venus' northern hemisphere. Orbital spacecraft radar observations of Venus culminated with the very successful *Magellan* mission in the early 1990s.

In the 1980s, the discovery of spectral windows allowed Earth-based IR observations of the subcloud atmosphere on Venus' nightside (Allen and Crawford, 1984). High-resolution IR spectroscopy in these windows led to the discovery of carbonyl sulfide (OCS) and the first measurements of HCl and HF below the clouds (Bézard *et al.*, 1990). The *Galileo* and *CASSINI* flybys of Venus (see Table 1) utilized these spectral windows to image the surface at near IR wavelengths.

Starting in the 1960s, Venus was the target of numerous spacecraft missions by the United States and the former Soviet Union. The major features of the successful missions are summarized in Table 1. Mission results, which have withstood the test of time and are relevant to Venusian geochemistry, are discussed in subsequent sections of this chapter.

One important point should be emphasized here. This is the paucity of spacecraft data on the chemical composition and thermal structure of Venus' lower atmosphere below ~22 km altitude (von Zahn *et al.*, 1983). About 80% of Venus' atmospheric mass is below this altitude. Furthermore, altitudes of 0–12 km span the region where the atmosphere is interacting with the surface. However, with three exceptions we have no data on the chemical composition of Venus' near-surface atmosphere. First is the older measurements of CO_2 and N_2 from crude chemical experiments on the *Venera 4–6* landers. Second, the water-vapor profile measured by the *Pioneer Venus* large probe neutral mass spectrometer. Third, the measurements of water-vapor and gaseous sulfur by spectrophotometer experiments on the *Venera 11–14* landers. The gas chromatograph and mass spectrometer experiments on

Table 1 Spacecraft missions to Venus.

Launch date	*Spacecraft*[a]	*Comments*
Aug. 27, 1962	Mariner 2, flyby	Dec. 14, 1962 flyby (36,000 km), confirmed high surface temp., 1st USA success; see *Space Sci. Rev.* **2**(6), 750–777, Dec. 1963
June 12, 1967	Venera 4, atm. probe	First successful atmospheric probe on Oct. 18, 1967 showed CO_2 is major gas; see Jastrow and Rasool (1969)
June 14, 1967	Mariner 5, flyby	Oct. 19, 1967 flyby (3,900 km), atmospheric structure & composition expts.; see Jastrow and Rasool (1969)
Jan. 5, 1969	Venera 5, probe	Venera 5 entry on May 16, 1969, failed at 26 km altitude
Jan. 10, 1969	Venera 6, probe	Venera 6 entry on May 17, 1969, failed at 11 km altitude; see *J. Atm. Sci.* **27**(7), July 1970, and Marov (1972)
Aug. 17, 1970	Venera 7, lander	Dec. 15, 1970, first soft landing on Venus, measured atmospheric composition, pressure, and temperature, survived 23 min (Marov, 1972)
Mar. 27, 1972	Venera 8, lander	July 22, 1972 landing, first analysis of surface: K, U, Th measured by γ-ray analysis, survived for 50 min
Nov. 3, 1973	Mariner 10, flyby	4,200 km flyby en route to Mercury on Feb. 5, 1974, IR, UV spectra, imaging of clouds, see *J. Atm. Sci.* **32**(6), June 1975, *Science* **183**(4131) 29 March 1974)
June 8, 1975	Venera 9, orbiter & lander	Orbit insertion on Oct. 20, 1975, landed Oct. 22, 1975, survived 53 min, first TV images of surface, γ-ray analysis of K, U, Th; see Hunten *et al.* (1983)
June 14, 1975	Venera 10, orbiter & lander	Orbit insertion on Oct. 23, 1975, landed Oct. 25, 1975, survived 65 min; see references for Venera 9.
May 20, 1978	Pioneer Venus 1,[b] orbiter	Orbit insertion Dec. 4, 1978, first radar mapping of another planetary surface, Venus atm. entry Aug. 1992
Aug. 8, 1978	Pioneer Venus 2,[b] bus & probes	Atm. entry Dec. 9, 1978 (bus, large probe, 3 small probes), first successful gc and ms analyses of atm
Sep. 9, 1978	Venera 11	Venera 11 flyby & probe entry Dec. 25, 1978,
Sep. 14, 1978	Venera 12, flybys & probes	Venera 12 flyby & probe entry Dec. 21, 1978, atmospheric science from 2 probes, no TV or surface analyses (Hunten *et al.*, 1983; Krasnopolsky 1986, papers in *Cosmic Res.* **17**(5) Sept./Oct. 1979)
Oct. 30, 1981	Venera 13, flyby & probe	Landed March 1, 1982, first color TV images and X-ray fluorescence analyses of surface, survived 127 min
Nov. 4, 1981	Venera 14, flyby & probe	Landed March 5, 1982, Venera 13 twin, survived 57 min; see *Cosmic Res.* **21**(2), Mar./Apr. 1983, Hunten *et al.* (1983), Krasnopolsky (1986), and Barsukov *et al.* (1992)
June 2, 1983	Venera 15, orbiter	Oct. 10, 1983, orbit entry.
June 7, 1983	Venera 16, orbiter	Oct. 14, 1983, orbit entry. Radar imaging from N. pole to 30° N, radar altimetry, and atm. spectroscopy expts. (Barsukov *et al.*, 1992; Bougher *et al.*, 1997)
Dec. 15, 1984	Vega 1, lander & balloon	Landed June 11, 1985, balloon flew 11,500 km at ~54 km in 46 h, lander survived 20 min
Dec. 21, 1984	Vega 2, lander & balloon	Landed June 15, 1985, balloon flew 11,000 km at ~54 km in 46 h, lander survived 20 min. Atmospheric science, XRF & γ-ray analyses of the surface; see *Cosmic Res.* **25**(5), Sept./Oct. 1987, Bougher *et al.* (1997), balloon papers in Science **231**, 21 March 1986.
May 4, 1989	Magellan, orbiter	Orbit insertion Aug. 10, 1990, radar mapping, altimetry, emissivity data for surface; radio occultation expts. atm. science, end of mission and loss of orbiter Oct. 12/13, 1994; see *J. Geophys. Res.* **97**, Aug. 25 & Oct. 25, 1992.
Oct. 18, 1989	Galileo, flyby	Feb. 10, 1990 flyby. Imaging & spectroscopy of atmosphere (Bougher *et al.*, 1997, papers in *Planet. Space Sci.* **41**(7), July 1993).
Oct. 15, 1997	CASSINI, flyby	First flyby Apr. 26, 1998, second flyby June 24, 1999, imaging & atmospheric science (Baines *et al.*, 2000).

Sources: Lodders and Fegley (1998) and National Space Science Data Center, Greenbelt, MD.
[a] US spacecraft: Mariner, Pioneer Venus, Magellan, Galileo, CASSINI. USSR spacecraft: Venera, Vega. [b] Pioneer Venus papers in *J. Geophys. Res.* **85**(A13), Dec. 30, 1980, *Icarus* **51**(2), Aug. 1982, *Icarus* **52**(2), Nov. 1982, Hunten *et al.* (1983) and Bougher *et al.* (1997).

the *Venera 11–14* and *Vega 1–2* landers did not return data from altitudes below 12 km (apparently by design). The atmospheric structure and net flux radiometer instruments on the *Pioneer Venus* large probe mysteriously failed at 12.5 km altitude. Current knowledge of the thermal structure of Venus' near-surface atmosphere is based upon crude pressure and temperature measurements from several of the early *Venera* landers, extrapolation of the *Pioneer Venus* measurements below 12.5 km, and more accurate data from the *Vega* 2 lander (Seiff, 1983; Crisp and Titov, 1997).

Table 1 lists key references that summarize results of the space missions. Jastrow and Rasool (1969) is a collection of *Mariner 5* and *Venera 4* papers. *Venus*, edited by Hunten *et al.* (1983), gives a detailed picture of Venus after the *Pioneer Venus* and *Venera 11–12* missions. Barsukov *et al.* (1992) report results of Soviet missions including the *Venera 13–14* probes, the *Venera 15–16* orbiters, and the *Vega 1–2* probes. *Venus II*, edited by Bougher *et al.* (1997), focuses on *Magellan* results relevant to geology, geophysics, and geochemistry of Venus. *Venus II* also describes results from the more recent Soviet missions (*Venera 13–14* onward) for atmospheric and surface chemistry.

Other books of interest include Lewis and Prinn (1984), which emphasizes the use of observational data for understanding the origin, evolution, and present-day chemistry of planetary atmospheres. Krasnopolsky (1986) focuses on chemistry of the atmospheres of Mars and Venus. He also reviews the atmospheric composition, thermal structure, and cloud measurements by the Soviet *Venera* and *Vega* missions. Chamberlain and Hunten (1987) is the classic text about chemistry and physics of planetary atmospheres. It describes results of the US and Soviet missions to Venus that are relevant to the composition, dynamics, and structure of Venus' atmosphere and ionosphere.

1.19.2 OVERVIEW OF IMPORTANT ORBITAL PROPERTIES

Several of Venus' orbital properties (summarized in Table 2) are unique and were not fully appreciated until the space age. Radar observations revealed that Venus' orbital period is ~224.70 d, and that its rotation period is 243.02 d (retrograde). Thus, a Venusian "day" is 116.75 Earth days long (1/day = 1/243.02 + 1/224.70), with the Sun rising in the west and setting in the east after 58.375 Earth days of daylight and rising again after another 58.375 Earth days of night. As shown by Shapiro *et al.* (1979), Venus' rotation period is close to, but clearly different from 243.16 d, which would be in 3 : 2 resonance with the Earth's orbital period. The orientation of Venus' spin axis is almost normal to the ecliptic with a tilt of ~177°. The relationship between the orbital periods of Venus and Earth is such that inferior conjunction (i.e., closest approach of the two planets) occurs once every 583.92 Earth days ($1/t$ = 1/224.70 − 1/365.25), at ~19 month intervals. As can be seen from Table 1, Soviet space missions to Venus during the 1960s were launched at similar intervals corresponding to successive inferior conjunctions. Finally, one should realize that Earth-based radar imaging and telescopic observations of Venus at inferior conjunction are of the same region of the planet because the 583.92 day synodic period is 5.001 Venusian days.

Table 2 Orbital and physical properties of Venus.

Property	*Value*	*Property*	*Value*
Semimajor axis (a, 10^6 km)	108.21	Mass (10^{24} kg)	4.8685
(AU)	0.7233	Modal radius (km)[d]	6,051.37
Perihelion (10^6 km)	107.48	Oblateness	0.0
Aphelion (10^6 km)	108.94	Volume (10^{10} km^3)	92.857
Orbital eccentricity (e)	0.0067	Mean density (kg m^{-3})	5,243
Inclination to the ecliptic (deg)	3.395	GM (10^{14} m^3 s^{-2})	3.2486
Sidereal orbital period (d)[a]	224.701	Mean gravity (m s^{-2})	8.870
Orbital obliquity (deg)	177.36	J_2 ($\times 10^6$)	4.4192
Tropical orbital period (d)[a]	224.695	Moment of inertia[e]	$0.331 \leq C/MR^2 \leq 0.341$
Mean orbital velocity (km s^{-1})	35.02	Solar constant (W m^{-2})	2,613.9
Synodic period (d)[b]	583.92	Bond albedo	0.750
Sidereal rotation period (d)[c]	−243.0185	Temperature at modal radius (K)[f]	740
Escape velocity (km s^{-1})	10.361	Pressure at modal radius (bar)[f]	95.6

After Lodders and Fegley (1998).

[a] The sidereal orbital period is the mean time for one revolution about the Sun relative to the fixed stars. The tropical orbital period is the mean time for one orbit from the same point to itself (such as equinox to equinox). [b] The time between Venus–Earth oppositions. [c] Retrograde rotation. [d] Median radius = 6,051.64 km, mean radius = 6,051.84 km. [e] Model-dependent constraint from Yoder (1997). [f] The temperature and pressure at the median and mean radii are 738.4 K, 94.5 bar and 736.8 K, 93.3 bar, respectively.

1.19.3 ATMOSPHERE

1.19.3.1 Composition

1.19.3.1.1 Basic definitions and general remarks

Throughout the rest of this chapter we discuss gas abundances using these three terms: volume-mixing ratio (henceforth mixing ratio), number density, and column density (or column abundance). The volume-mixing ratio is a dimensionless quantity also called the mole (or volume) fraction of a gas, and is the gas partial pressure (P_i) divided by the total pressure (P_T). Mixing ratios are given in percent for major gases and as parts per million, per billion, or per trillion by volume (ppmv, ppbv, or pptv) for trace gases.

The number density of a gas i is denoted by square brackets $[i]$ and has the dimensions of particles (atoms plus molecules) per unit volume, e.g., particles cm^{-3}. It is equal to either $P_i N_A/RT$ or P_i/kT, where N_A is Avogadro's number, R is the ideal gas constant, k is Boltzmann's constant, and T is temperature in kelvin. For reference, the number density of Earth's atmosphere is 2.55×10^{19} particles cm^{-3} at sea level, where $T = 288.15$ K and $P = 1$ atm. The number density of Venus' atmosphere is 9.36×10^{20} particles cm^{-3} at 0 km, where $T = 740$ K and $P = 95.6$ bar. The 0 km level on Venus is the modal radius (see Table 2).

The column abundance of a gas is the number of gas particles throughout an atmospheric column and has the dimensions of particles per unit area, e.g., particles cm^{-2}. The column abundance is thus the integral of $[i]dz$ from a specified altitude z_0, such as the planetary surface, to the top of the atmosphere ($z =$ infinity). The column density can also be calculated from $P_i N_A/gM$, where M is the formula weight of the gas and g is the gravitational acceleration as a function of altitude. Note that the total atmospheric mass per unit area is simply P_T/g. The mean molecular weight, column density, and column mass of the terrestrial atmosphere are 28.97 g mol^{-1}, 2.15×10^{25} particles cm^{-2}, and 1,034.2 g cm^{-2} at sea level. The corresponding values for Venus' atmosphere are 43.46 g mol^{-1}, 1.49×10^{27} particles cm^{-2}, and 107,531 g cm^{-2} at 0 km.

The chemical composition of Venus' atmosphere is described below. This discussion is based on sources listed in Table 3, Fegley and Treiman (1992), and Warneck (1988).

As shown in Table 3, Venus' atmosphere is dominantly CO_2 (96.5%) and N_2 (3.5%), with smaller amounts of SO_2, H_2O, CO, OCS, HCl, HF, the noble gases, and reactive species such as SO that are produced photochemically. The abundances of CO_2, N_2, the noble gases, HCl, and HF are apparently constant throughout most of Venus' atmosphere, but other gases such as SO_2, H_2O, CO, OCS, and SO have spatially and temporally variable abundances. Variations in the abundances of water vapor, CO, and sulfur gases are of particular interest because they result from the solar UV-driven photochemistry that maintains the global sulfuric acid cloud cover.

In addition to the gases listed in Table 3, Earth-based and spacecraft microwave spectroscopy indicates that H_2SO_4 vapor (with a mixing ratio of several tens of ppmv) is present below the clouds. Sulfur trioxide, as yet unobserved, is also expected to be present below the clouds in equilibrium with H_2SO_4 vapor. Spectrophotometers on *Venera 11–14* found absorption of blue sunlight in Venus' lower atmosphere. This is attributed to elemental sulfur vapor with a total mixing ratio (for all allotropes) of ~20 ppbv in Venus' lower atmosphere.

1.19.3.1.2 Carbon, sulfur, and halogen gases

The high atmospheric abundances of CO_2, SO_2, OCS, HCl, and HF on Venus are due to the high temperatures at Venus' surface (Fegley and Treiman, 1992). All these gases are present at much lower abundances in the Earth's atmosphere. For example, average mixing ratios in the terrestrial troposphere of CO_2, SO_2, OCS, HCl, and HF are 360 ppmv, 20–90 pptv, 500 pptv, ~1 ppbv, and ~25 pptv, respectively (cf. Table 3). Also the major sources and sinks for these gases on Earth are different from their probable sources and sinks on Venus.

Volcanic outgassing is probably the major source of CO_2 in Venus' atmosphere. Above the clouds CO_2 is converted to CO and O_2 by photolysis (see Section 1.19.3.3), while carbonate formation may be an important sink at the surface. In contrast, CO_2 in Earth's atmosphere has anthropogenic, biogenic, and geological sources with estimates indicating pre-industrial CO_2 levels of 290 ppmv or less. The major sinks are biogenic (i.e., consumption by photoautotrophs), dissolution in the oceans, and rock weathering (acting over longer timescales than the first two sinks). The column density of CO_2 in Earth's atmosphere is $\sim 5.1 \times 10^{21}$ molecules cm^{-2}, which is $\sim 2.75 \times 10^5$ times lower than on Venus. However, the crustal carbon inventory on Earth is about the same as the CO_2 column density on Venus ($\sim 0.7 \times 10^{27}$ C atoms cm^{-2} for crustal carbon on Earth versus 1.4×10^{27} CO_2 molecules cm^{-2} on Venus). Does this similarity mean that all CO_2 on Venus has been degassed and is now in the atmosphere? The short answer is that we do not know. We consider the related questions of whether or not carbonates exist on Venus' surface and whether or not the atmospheric abundances of CO_2, SO_2, OCS, HCl,

Table 3 Chemical composition of the atmosphere of Venus.

Gas	*Abundance*[a]	*Source(s)*	*Sink(s)*
CO_2	96.5 ± 0.8%	Outgassing	Carbonate formation
N_2	3.5 ± 0.8%	Outgassing	
SO_2[b]	150 ± 30 ppm (22–42 km) 25–150 ppm (12–22 km)	Outgassing and reduction of OCS, H_2S	H_2SO_4 formation and $CaSO_4$ formation
H_2O[b]	30 ± 15 ppm (0–45 km) 30–70 ppm (0–5 km)	Outgassing	H escape and Fe^{2+} oxidation
^{40}Ar	31^{+20}_{-10} ppm	Outgassing (^{40}K)	
^{36}Ar	30^{+20}_{-10} ppm	Primordial	
CO[b]	45 ± 10 ppm (cloud top) 30 ± 18 ppm (42 km) 28 ± 7 ppm (36–42 km) 20 ± 3 ppm (22 km) 17 ± 1 ppm (12 km)	CO_2 photolysis	Photo-oxidation to CO_2
^4He[c]	0.6–12 ppm	Outgassing (U, Th)	Escape
Ne	7 ± 3 ppm	Outgassing, primordial	
^{38}Ar	5.5 ppm	Outgassing, primordial	
OCS[b]	4.4 ± 1 ppm (33 km)	Outgassing and sulfide weathering	Conversion to SO_2
H_2S[b]	3 ± 2 ppm (<20 km)	Outgassing and sulfide weathering	Conversion to SO_2
HDO[b]	1.3 ± 0.2 ppm (subcloud)	Outgassing	H escape
HCl	0.6 ± 0.12 ppm (cloud top) 0.5 ppm (35–45 km)	Outgassing	Cl-mineral formation
^{84}Kr	25^{+13}_{-18} ppb	Outgassing, primordial	
SO[b]	20 ± 10 ppb (cloud top)	Photochemistry	Photochemistry
S_{1-8}[b]	20 ppb (<50 km)	Sulfide weathering	Conversion to SO_2
HF	$5^{+5}_{-2.5}$ ppb (cloud top) 4.5 ppb (35–45 km)	Outgassing	F-mineral formation
^{132}Xe	<10 ppb	Outgassing, primordial	
^{129}Xe	<9.5 ppb	Outgassing (^{129}I)	

Sources: Lodders and Fegley (1998) and Wieler (2002).
[a] Abundance by volume, ppm = parts per million, ppb = parts per billion, e.g., 4.5 ppb is a volume mole fraction of 4.5×10^{-9}.
[b] Abundances of these species are altitude dependent (see text). [c] The He abundance in Venus' upper atmosphere where diffusive separation occurs is 12^{+24}_{-6} ppm by volume (von Zahn *et al*., 1983). The lower atmospheric value listed above is a model-dependent extrapolation.

and HF are regulated or buffered by mineral assemblages on Venus' surface in Section 1.19.4.2.

Carbon monoxide is the second most abundant carbon-bearing gas in Venus' atmosphere. The CO abundance in Venus' lower atmosphere is altitude dependent and decreases toward the surface as follows: 45 ± 10 ppmv (~64 km), 30 ± 18 ppmv (42 km), 20 ± 3 ppmv (22 km), and 17 ± 1 ppmv (12 km). This gradient is consistent with photochemical production of CO from CO_2 in Venus' upper atmosphere and CO consumption by thermochemical reactions with sulfur gases in Venus' lower atmosphere and with minerals at its surface. Carbon monoxide is also photo-oxidized back to CO_2 via catalytic cycles that are described in Section 1.19.3.3.

By comparison, the average CO mixing ratio in Earth's troposphere is ~0.12 ppmv and it is produced from a variety of anthropogenic and biogenic sources such as fossil fuel combustion, biomass burning, and oxidation of methane and other hydrocarbons. Most of the CO in Earth's troposphere is destroyed by reaction with OH radicals, which are also important for the catalytic reformation of CO_2 on Venus under some conditions.

Sulfur dioxide is the most abundant sulfur-bearing gas, and the third most abundant gas after CO_2 and N_2 in Venus' lower atmosphere. The SO_2 mixing ratio below the clouds is ~150 ppmv, as measured by gas chromatographs on the *Pioneer Venus* and *Venera 11–12* atmospheric entry probes. Its abundance varies with altitude and may also be temporally variable. Volcanic outgassing of SO_2 and outgassing and subsequent oxidation of reduced sulfur gases (OCS and H_2S) are probably the major sources of SO_2 on Venus. Photochemical oxidation to aqueous sulfuric acid droplets efficiently removes SO_2 from Venus' upper atmosphere (cf. ~150 ppmv below the clouds versus ~10 ppbv above the clouds). Reduction of SO_2 to OCS and reaction of SO_2 with calcium-bearing minerals to form anhydrite ($CaSO_4$) may be important sinks for SO_2 in the near-surface atmosphere.

In contrast to Venus, SO_2 is only a trace gas in Earth's atmosphere and it is generally less abundant than OCS and other reduced sulfur gases in Earth's troposphere. The average SO_2

column abundance in the terrestrial atmosphere is $\sim 4 \times 10^{15}$ molecules cm^{-2} versus a column abundance of $\sim 2.2 \times 10^{23}$ molecules cm^{-2} in Venus' atmosphere. The total amount of sulfur in Earth's oceans and crust is ~600 times larger than the SO_2 column abundance on Venus, which probably does not represent the planet's total sulfur inventory. Most of the SO_2 in the terrestrial troposphere is anthropogenic with volcanic emissions being one to two orders of magnitude less important. Sulfur dioxide is removed from Earth's troposphere by oxidation to sulfate, which occurs via photochemical and thermochemical processes in the gas phase, in cloud droplets, and on particulates.

Carbonyl sulfide is the most abundant reduced sulfur gas in Venus' subcloud atmosphere. The OCS mixing ratio is 4.4 ± 1.0 ppmv at 33 km altitude. Earth-based IR spectroscopy shows that the OCS mixing ratio increases with decreasing altitude in the 26–45 km range. Extrapolation of this gradient indicates that the OCS abundance may reach tens of ppmv at Venus' surface. The increase in OCS may be balanced by a decrease in SO_2 at low altitudes, such as that reported by UV spectrometers on the *Vega 1* and *2* probes. However, the 2.3 μm spectroscopic window used to observe OCS only probes altitudes in the 26–45 km range, and the *Vega* UV spectrometer data are difficult to understand. Thus, the gradients in the OCS and SO_2 abundances in the lowest 20 km of Venus' atmosphere require confirmation. Theoretical models and laboratory studies indicate that the major sources of OCS on Venus are probably volcanic outgassing and chemical weathering of iron sulfide minerals such as pyrrhotite (ranging in composition from FeS to Fe_7S_8). The major sink for OCS is photochemical oxidation to SO_2. Some OCS may also be lost by reaction with monatomic S to form CO and S_2 vapor.

Carbonyl sulfide is also the most abundant reduced sulfur gas in Earth's troposphere, but for completely different reasons. Volcanic sources of OCS are negligible by comparison with biogenic emissions, which are important sources of several reduced sulfur gases (e.g., OCS, H_2S, $(CH_3)_2S$, $(CH_3)_2S_2$, and CH_3SH) in the terrestrial troposphere. Many of these gases are ultimately converted into sulfate aerosols in the troposphere, but OCS is mainly lost by transport into the stratosphere, where it is photochemically oxidized to SO_2 and then to sulfuric acid aerosols, which form the Junge layer at ~20 km in Earth's stratosphere.

Volcanic outgassing is plausibly the major source of HCl and HF in Venus' atmosphere. Thermochemical equilibrium calculations suggest that formation of chlorine- and fluorine-bearing minerals are important sinks for these two gases. Observations by Connes *et al.* (1967) and Bézard *et al.* (1990) give the same HCl and HF mixing ratios, within error, of ~0.5 ppmv and ~5 ppbv above and below the clouds, respectively. The column densities of $\sim 7 \times 10^{20}$ HCl molecules cm^{-2} and $\sim 7 \times 10^{18}$ HF molecules cm^{-2} in Venus' atmosphere are many orders of magnitude greater than the column densities of $\sim 2 \times 10^{16}$ HCl molecules cm^{-2} and $\sim 5 \times 10^{14}$ HF molecules cm^{-2} in Earth's troposphere. Furthermore, most of the 25 pptv HF, and some of the 1 ppbv HCl in the terrestrial troposphere are from anthropogenic sources, and not from volcanic emissions. Tropospheric HF is mainly from industrial emissions and downward mixing from the stratosphere, where it forms as a result of photolytic destruction of synthetic chlorofluorocarbon (CFC) gases. The HCl originates from sea salt, volcanic gases, and from HCl mixed downward from the stratosphere, where it is produced from photolysis of CFC gases. However, most of the fluorine and chlorine in Earth's troposphere are in CFC gases with only minor amounts in HF and HCl.

1.19.3.1.3 Water vapor

Venus' atmosphere is so dry that Earth-based and spacecraft measurements of the water-vapor abundance are extremely difficult. Historically, many of the *in situ* water-vapor measurements gave values much higher than the actual water-vapor content. However, reliable values are now available from several sources including the *Pioneer Venus* mass spectrometer, spectrophotometer experiments on *Venera 11–14*, Earth-based FTIR spectroscopy of Venus' lower atmosphere on the nightside, and IR observations during the *Galileo* and *Cassini* flybys of Venus.

The average water-vapor mixing ratio below the clouds is ~30 ppmv. In comparison, the terrestrial troposphere has water-vapor mixing ratios of 1–4%. Although it is a trace gas, water vapor is the major reservoir of hydrogen in Venus' subcloud atmosphere, and is an important reactant in chemical reactions that are hypothesized to buffer or regulate the atmospheric abundances of HCl and HF. The loss of water from Venus, via oxidation of the surface and hydrogen escape to space, ultimately regulates the oxidation state of the atmosphere and surface. Furthermore, the high D/H ratio in atmospheric water vapor suggests that Venus was once wet, with the equivalent of a global ocean at least 4 m and possibly 530 m deep (Donahue *et al.*, 1997).

A long-standing question is whether or not the water-vapor abundance in Venus' lower atmosphere varies with altitude. Initial interpretation of spectrophotometer experiments on the *Venera 11–14* spacecraft suggested a monotonic decrease from ~200 ppmv at 50 km to ~20 ppmv at the

surface. However, most of the measurements mentioned above now indicate a constant mixing ratio of 30 ± 15 ppmv throughout the lower atmosphere. Even though Venus is drier than Earth, volcanic emissions are the plausible major source of atmospheric water vapor. A major (reversible) sink is formation of the aqueous sulfuric acid clouds. Another sink, that is irreversible, and occurs on longer timescales, is reaction of water vapor with ferrous iron minerals on Venus' surface to form ferric iron minerals and hydrogen gas. The H_2 gas is then dissociated to hydrogen atoms in Venus' upper atmosphere and lost to space.

Venus' upper atmosphere is even drier than the lower atmosphere, and the average water-vapor mixing ratio above the clouds is only a few ppmv. The very low H_2O mixing ratios were hard to explain until it was realized that Venus' clouds are 75% sulfuric acid, which is a powerful drying agent. When dissolved in the acid, most of the water reacts with H_2SO_4 to form hydronium (H_3O^+) and bisulfate (HSO_4^-) ions. As a result, the concentrations of "free" H_2O in the acid solution and in the vapor over the acid are extremely low. The partial pressure of water at Venus' cloud tops is lower than that over water ice at the same temperature. Thus, the clouds are responsible for the extreme dryness of Venus' upper atmosphere, and play an important role in the photochemical stability of Venus' atmosphere (see Section 1.19.3.3).

1.19.3.1.4 Nitrogen and noble gases

Although N_2 is the second-most abundant gas in Venus' atmosphere, measurements of its abundance are difficult. The mass spectrometers on *Pioneer Venus* and *Venera 11–12* gave N_2 mixing ratios of 4% at ~22 km, but the gas chromatograph (GC) experiments on the same spacecraft gave different values. For example, the *Venera 11–12* GC reported 2.5 ± 0.3% in the 22–42 km region, while the *Pioneer Venus* GC reported an altitude-dependent N_2 mixing ratio of 3.4% at 22 km, 3.54% at 42 km, and 4.6% at 52 km. The GC data are difficult to explain. The recommended value of 3.5 ± 0.8% for the N_2 abundance reflects the disagreements between the mass spectrometer and GC results (von Zahn *et al.*, 1983).

Volcanic outgassing is probably the major source of N_2, and formation of nitrogen oxides (NO_x) by lightning may be a sink for N_2 on Venus. The timescales for both of these processes are uncertain, but are plausibly very long.

Ultimately, Earth's N_2 is probably also due to volcanic emissions. At present, the major N_2 sources are denitrifying bacteria in soils and in the oceans. The major N_2 sinks on Earth are nitrogen-fixing bacteria in soils and the oceans. These sources and sinks result in a lifetime of ~17 Myr for atmospheric N_2 on Earth. If the biological sources and sinks were removed, while lightning and forest fires continued at their present rates, the lifetime for atmospheric N_2 would increase to ~80 Myr. However, in the absence of biology, Earth's atmosphere would contain much less O_2, so combustion and lightning would be much less efficient sinks for nitrogen. In this case N_2 would have a lifetime of ~1 Gyr.

The observed noble-gas abundances and isotopic ratios on Venus are summarized in Tables 3 and 4. The helium mixing ratio is a model-dependent extrapolation of the value measured in Venus' upper atmosphere, where diffusive separation of gases occurs. The main differences between Venus and Earth are that Venus is apparently richer in ^{4}He, ^{36}Ar, and ^{84}Kr than the Earth, and the low ^{40}Ar/^{36}Ar ratio of ~1.1 on Venus, which is ~270 times smaller than on Earth. The low ^{40}Ar/^{36}Ar ratio may reflect more efficient solar-wind implantation of ^{36}Ar in solid grains accreted by Venus and/or efficient early outgassing that then stopped due to the lack of plate tectonics. Wieler (2002) discusses the noble-gas data. Volkov and Frenkel (1993) and Kaula (1999) describe implications of the ^{40}Ar/^{36}Ar ratio for outgassing of Venus.

1.19.3.1.5 Isotopic composition

Table 4 summarizes the data on the isotopic composition of Venus' atmosphere. Aside from the noble gases, the most important difference between Venus and Earth is the high D/H ratio, which is ~150 times greater than the D/H ratio of 1.558×10^{-4} in standard mean ocean water (SMOW). The high D/H ratio strongly suggests,

Table 4 Isotopic composition of Venus' atmosphere.

Isotopic ratio[a]	*Observed value*	*Method*
D/H	0.016 ± 0.002	Pioneer Venus (PV) MS[b]
	0.019 ± 0.006	IR spectroscopy
^{3}He/^{4}He	$<3 \times 10^{-4}$	PV MS
^{12}C/^{13}C	86 ± 12	IR spectroscopy
	88.3 ± 1.6	Venera 11/12 MS
^{14}N/^{15}N	273 ± 56	PV MS
^{16}O/^{18}O	500 ± 25	PV MS
	500 ± 80	IR spectroscopy
^{20}Ne/^{22}Ne	11.8 ± 0.6	Venera 11/12 MS
^{21}Ne/^{22}Ne	<0.067	Venera 11/12 MS
^{35}Cl/^{37}Cl	2.9 ± 0.3	IR spectroscopy
^{36}Ar/^{38}Ar	5.45 ± 0.1	PV, Venera 11/12 MS
^{40}Ar/^{36}Ar	1.11 ± 0.02	PV, Venera 11/12 MS

Sources: Lodders and Fegley (1998) and Wieler (2002).
[a] No isotopic compositions are available for Kr and Xe on Venus.
[b] MS = mass spectrometer.

but does not prove, that Venus had more water and has lost most of it over time. This deduction is based on the assumption that Venus initially had the same D/H ratio as Earth. However, a wide range of D/H ratios are observed in other planets, meteorites, interplanetary dust particles (IDPs), and in comet P/Halley, so this assumption may be incorrect.

The carbon, nitrogen, oxygen, and chlorine isotopic ratios are the same as the terrestrial values, within rather large uncertainties. However, any difference in the oxygen isotopic composition of Venus and Earth is probably only a few parts per thousand (or less) and cannot be resolved from the present data. The isotopic ratios of the three stable oxygen isotopes (16, 17, 18) are of most interest because of the known variations in meteorites and IDPs and because oxygen is either the first or second (after iron) most abundant element in a rocky planet. However, the ^{17}O isotopic abundance has not been measured on Venus. This could be done using isotopic bands of CO_2 (e.g., see Bézard *et al.*, 1987), although probably with uncertainties of ~10%. It is important to measure abundances of the three oxygen isotopes (with an uncertainty of <0.1‰) on Venus to see if it has the same oxygen isotopic composition as the Earth and Moon. Accurate measurements of oxygen, hydrogen, carbon, and sulfur isotopic ratios in gases in Venus' upper atmosphere are desirable, because photochemical reactions plausibly cause variations in these ratios, e.g., as seen with mass-independent variations in oxygen-bearing gases in Earth's atmosphere and in some nitrate and sulfate minerals on Earth.

1.19.3.2 Thermal Structure and Greenhouse Effect

Venus has the highest albedo of any planet (e.g., 0.75 versus 0.29 for Earth). Even though the solar constant at Venus (2613.9 W m^{-2}) is ~1.9 times larger ($=1/0.723^2$) than that at Earth, Venus absorbs only ~66% as much solar energy, i.e., ~160 W m^{-2} versus 243 W m^{-2}, as Earth. The energy deposition is dramatically different from that on Earth, where ~66% of the absorbed solar energy is deposited at the surface. In contrast, ~70% of the absorbed sunlight is deposited in Venus' upper atmosphere and clouds, another 19% is deposited in the lower atmosphere, and only ~11% reaches the surface. The "sunlight" at Venus' surface is ~5 times dimmer than that on Earth.

The high temperature and pressure at Venus' surface (740 K and 95.6 bar at the modal radius of 6,051.4 km) are due to a super-greenhouse effect maintained by the high IR opacity of CO_2, SO_2, and H_2O in its lower atmosphere. The origin, duration, and present stability of the Venusian super-greenhouse remain somewhat of a mystery. One problem is finding enough IR opacity to maintain the greenhouse. The earlier greenhouse models used the large water-vapor mixing ratios (1,000 ppmv or higher) indicated by the *Venera 4–6* probes and Earth-based microwave sounding of the subcloud atmosphere. However, we now know that the water-vapor mixing ratio below Venus' clouds is ~30 ppmv. Another problem is an incomplete knowledge of IR opacities of CO_2, SO_2, H_2O, and other possible greenhouse gases at the high temperatures and high pressures prevailing in Venus' lower atmosphere. Finally, proper incorporation of the clouds into greenhouse modeling is yet another problem. Crisp and Titov (1997) review the state of the art in modeling the Venusian greenhouse and present current ideas for addressing these problems.

Figure 1 shows the temperature and pressure profiles from 0 km to100 km altitude in Venus' atmosphere. The 0–60 km region is the troposphere, the 60–100 km region on the dayside or the 60–160 km region on the nightside is the mesosphere (sometimes also called the stratomesosphere), the 100–160 km region on the dayside is the thermosphere, and the exosphere is above 160 km. The latter regions are discussed in Section 1.19.3.5.

There are several key differences between the atmospheres of Venus and Earth. The terrestrial atmosphere has a pronounced temperature inversion at the tropopause, which is the boundary between the troposphere and the stratosphere. This inversion is due to absorption of UV sunlight by ozone, but is absent on Venus, which has too little O_2 (<0.3 ppmv) to form an ozone layer. The temperature gradient of ~8 K km^{-1} in Venus' troposphere is very close to the dry (i.e., condensation cloud free) adiabatic gradient. This is

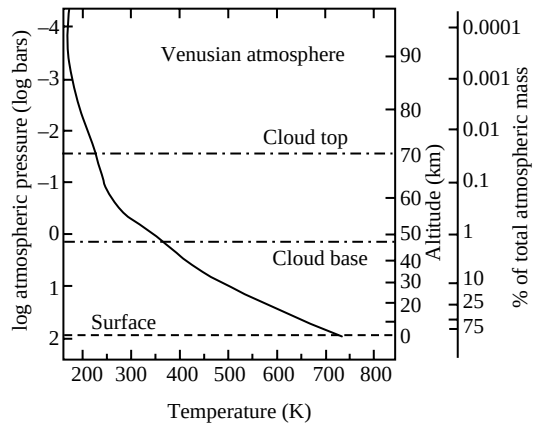

Figure 1 Temperature and pressure as a function of altitude in Venus' atmosphere. The position of the global clouds is also indicated.

given by $dT/dz = -gM/C_P = -g/c_p$, where C_P and c_p are the average molar heat capacity and specific heat, respectively, of Venus' atmosphere (96.5% CO_2 + 3.5% N_2). In contrast, the average temperature gradient in Earth's troposphere is ~6.5 K km^{-1}, significantly subadiabatic compared to the dry adiabatic gradient of ~10 K km^{-1} for air. The discrepancy is caused by water cloud condensation in Earth's troposphere, which releases the latent heat of vaporization (or sublimation) and thus warms the surrounding gas. The average surface temperature on Venus is ~450 K higher than the average surface temperature of 288 K on Earth. Analysis of the available temperature and wind-speed measurements indicates that meridional temperature gradients on Venus' surface are only a few degrees compared to ~50 K on Earth. However, *in situ* temperature measurements only extend to 60° N latitude on Venus. Temperatures on Venus' surface vary with altitude. The temperature is ~648 K and pressure is ~43 bar at the top of Maxwell Montes, which is ~12 km above the modal radius of 6,051.4 km and is the highest point on the planet.

1.19.3.3 Clouds and Photochemical Cycles

The most prominent feature of Venus' middle atmosphere is the global cloud layer that begins at ~45 km altitude and extends to ~70 km altitude, with thinner hazes ~20 km above and below these altitudes. Venus appears yellow-white in visible light, but the first UV images of Venus in the 1920s showed dark $\mathscr{Y}$- or $\mathscr{V}$-shaped cloud features. The features are formed by an unknown UV absorber that absorbs about half of all sunlight deposited in the clouds at wavelengths ≤500 nm. The UV absorber may be elemental sulfur, Cl_2, an S–Cl gas, chlorine compounds dissolved in cloud droplets, or another sulfur gas.

All of the clouds are low density, because the visibility inside the densest region of the clouds is a few kilometers. The average and maximum optical depths (τ) in visible light of all cloud layers are 29 and 40, respectively, versus average and maximum τ values of 6 and ~350 for terrestrial clouds. Average mass densities for Venus' clouds are 0.01–0.02 g m^{-3} versus an average mass density of 0.1–0.5 g m^{-3} for fog clouds on Earth. Venus' cloud layers are typically divided into the subcloud haze (32–48 km), the lower cloud (48–51 km), middle cloud (51–57 km), upper cloud (57–70 km), and upper haze (70–90 km).

Nephelometers, which use scattered light to measure particle size and number density, on *Venera 9–11* and *Pioneer Venus* showed that the cloud layers are composed of three different types of particles. The first type are aerosols of ~0.3 μm diameter (mode-1 particles), which occur in the upper and middle clouds. The second type are spherical droplets of ~2 μm diameter (mode-2 particles) composed of 75% sulfuric acid ($H_2SO_4 \cdot 2H_2O$), which occur throughout the clouds. The third type are the mode-3 particles with ~7 μm diameter, which have an unknown composition, and occur in the middle to lower clouds. By comparison, fog clouds on the Earth are composed of droplets with diameters of 0.5–30 μm. Aqueous sulfuric acid droplets comprise the visible clouds seen from Earth. The mode-1 and mode-3 particles may also be sulfuric acid particles. Some data suggest that the mode-3 particles may be crystalline and could be composed of iron or aluminum chlorides, solid perchloric acid hydrates, or phosphorus oxides.

The aqueous sulfuric acid droplets in the clouds result from UV sunlight photolysis of SO_2, which reduces the SO_2 abundance from ~150 ppmv below the clouds to ~10 ppbv at the cloud tops. The photochemistry of SO_2 and CO_2 is closely coupled. The O_2 produced from CO_2 photolysis is used to convert SO_2 to SO_3, which then forms sulfuric acid. Spectroscopic observations show temporal trends in the SO_2 abundance at the cloud tops. These observed variations are probably due to atmospheric dynamics.

The CO_2 in Venus' atmosphere (like CO_2 on Mars) is continually converted by UV sunlight to oxygen and CO:

$$CO_2 + h\nu \rightarrow CO + O(^3P) \quad (\lambda < 227.5\ \text{nm}) \qquad (1)$$

$$\rightarrow CO + O(^1D) \quad (\lambda < 167.0\ \text{nm}) \qquad (2)$$

The electronically excited (^1D) oxygen atoms formed in reaction (2) are rapidly converted to the ground state (^3P) by collisions with other molecules. The direct recombination of oxygen atoms and CO

$$CO + O(^3P) + M \rightarrow CO_2 \qquad (3)$$

where M is any gas, is forbidden by quantum mechanical spin selection rules, and is much slower than oxygen atom recombination to form O_2:

$$O(^3P) + O(^3P) + M \rightarrow O_2 + M \qquad (4)$$

Photolysis would completely destroy all CO_2 above the clouds in ~1.4×10^4 yr and all CO_2 in Venus' atmosphere in ~5 Myr. In addition, CO_2 photolysis would produce observable amounts of O_2 in ~5 yr unless CO_2 is reformed by another route. However, O_2 is not seen in Venus' atmosphere and the spectroscopic upper limit is <0.3 ppmv. Gas-phase catalytic reformation of CO_2 by hydrogen, chlorine, or nitrogen gases has been proposed to solve this problem. The relative importance of the catalytic schemes depends on the H_2 abundance in Venus'

strato-mesosphere, which is unknown, because H_2 is involved in chemistry forming OH radicals. For example, the reaction

$$CO + OH \rightarrow CO_2 + H \quad (5)$$

is important at H_2 levels of tens of ppmv. At very low H_2 levels of ~0.1 ppbv, reaction (5) is no longer important and catalytic cycles such as

$$CO + Cl + M \rightarrow COCl + M \quad (6)$$

$$COCl + O_2 + M \rightarrow ClCO_3 + M \quad (7)$$

$$ClCO_3 + O \rightarrow CO_2 + O_2 + Cl \quad (8)$$

$$\text{Net: } CO + O \rightarrow CO_2 \quad (9)$$

$$CO + Cl + M \rightarrow COCl + M \quad (6)$$

$$COCl + O_2 + M \rightarrow ClCO_3 + M \quad (7)$$

$$ClCO_3 + Cl \rightarrow CO_2 + ClO + O \quad (10)$$

$$ClCO_3 + O \rightarrow CO_2 + O_2 + Cl \quad (8)$$

$$\text{Net: } CO + O \rightarrow CO_2 \quad (9)$$

recycle CO to CO_2. At intermediate H_2 levels of ~0.1 ppmv, the reaction

$$NO + HO_2 \rightarrow NO_2 + OH \quad (11)$$

precedes reaction (5), which then recycles CO to CO_2. Yung and DeMore (1982) and Krasnopolsky (1986) give detailed discussions of Venusian atmospheric photochemistry. More recent work is described by Esposito *et al.* (1997) and by Mills (1998).

1.19.3.4 Atmospheric Dynamics

The major feature of atmospheric dynamics on Venus is that above ~16 km, i.e., above the first scale height ($H = RT/gM$), the atmosphere rotates much faster than the planet itself. The atmospheric zonal rotation is retrograde and reaches a maximum velocity of ~100 m s^{-1} at the cloud tops (70 km). Tracking of the UV-dark features in the clouds, first from Earth-based observations by Boyer and Carmichel in the 1960s and later from observations by *Pioneer Venus* and *Mariner 10*, showed the high-speed retrograde zonal winds known as the four-day super-rotation. *In situ* measurements by Doppler tracking of the *Pioneer Venus*, *Venera*, and *Vega* entry probes show that the zonal winds decrease with decreasing altitude and are ~1 m s^{-1} or less at the surface. The origin of the four-day super-rotation is still incompletely understood, and our present understanding is reviewed by Gierasch *et al.* (1997).

1.19.3.5 Upper Atmosphere and Solar-wind Interactions

Venus' ionosphere is the upper atmospheric region, where significant ion and electron densities exist. It coexists with the thermosphere and exosphere. The electrons and ions in Venus' dayside ionosphere are primarily formed by extreme solar UV photoionization of neutral gases in the thermosphere. However, CO_2^+, like N_2^+ on Earth, is only a minor ion in the ionosphere. The major species in Venus' lower ionosphere is O_2^+ with a maximum number density of ~10^6 cm^{-3}. The CO_2^+/O_2^+ ratio is less than 10%. Above 200 km O^+ is the major ion. The maximum electron density is ~3×10^5 cm^{-3} at ~140 km altitude. The solar wind directly interacts with the upper atmosphere, because Venus does not have a magnetic field. This interaction terminates the ionosphere at the ionopause, which is typically at 400–500 km. However, the ionopause level is variable. The nightside ionosphere is formed by flow of ionospheric plasma from the dayside of the planet. The maximum ion densities on the nightside are 10^4 cm^{-3}. Fox and Kliore (1997), Nagy and Cravens (1997), and Kasprzak *et al.* (1997) discuss Venus' ionosphere and upper atmospheric interactions with the solar wind in more detail.

1.19.4 SURFACE AND INTERIOR

1.19.4.1 Geochemistry and Mineralogy

Our knowledge of the geochemistry and mineralogy of Venus' surface primarily comes from six types of information: (i) elemental analyses of several major elements by X-ray fluorescence (XRF) spectroscopy; (ii) analyses of potassium, uranium, and thorium by γ-ray spectroscopy; (iii) TV imaging from several *Venera* landers; (iv) Earth-based and spacecraft radar observations of the dielectric constant and morphology of the surface (Pettengill *et al.*, 1997); (v) models of thermochemical equilibria between atmospheric gases and presumed crustal minerals; and (vi) laboratory studies of the rates of reactions that are sinks or sources of sulfur-bearing gases. However, it is important to emphasize that we have no direct knowledge of the mineralogy of Venus' surface because there are no X-ray diffraction (XRD) measurements or other data that would unambiguously identify the minerals present.

Table 5 lists the seven *Venera* and *Vega* space probes that made elemental analyses of the surface of Venus. In addition to elemental analyses, several of the *Venera* and *Vega* landers measured density, bearing capacity, electrical resistivity, and atmospheric redox state (via the reaction of chemically impregnated asbestos with atmospheric CO). The *Venera 8–10*, and *Vega 1–2* probes analyzed

Table 5 Geochemical analyses and imaging on the surface of Venus.

Probe	°*Lat*[a]	°*Long*[a]	*Alt.* (km)[b]	*Location and suggested rock types*[c]	*Experiment*
Venera 8	−10.7	335.25	0.5 ± 0.2	Mottled volcanic plains E. of Navka Planitia; leucitite, lamprophyres, rhyolite, γ-ray density = 2.8 ± 0.1 g cm^{-3}	γ-ray
Venera 9	31.0	291.64	1.3 ± 0.5	N.E. slope of Beta Regio, lander site has15° to 20° slope with decimeter-size rock fragments with soil between them, E-MORB-like basaltic tholeiite	γ-ray, TV image,[d] photometry[e]
Venera 10	15.42	291.51	0.8 ± 0.6	Lowlands near SE edge of Beta Regio, lander site has soil between 10–15 cm high outcrops of bedrock, N-MORB-like basaltic tholeiite	γ-ray, TV image,[d] photometry[e]
Venera 13	−7.55	303.69	0.8 ± 0.3	Navka Planitia at E. end of Phoebe Regio rise, landscape similar to Venera 10 site, mafic alkaline rocks such as weathered olivine leucitite, nephelinite, volume density = 1.4–1.5 g cm^{-3} from impact loading	XRF, redox expt., TV imaging,[d,e] impact load
Venera 14	−13.05	310.19	0.9 ± 0.3	S. Navka Planitia on flank of a volcano, landing site is a plain dominated by layered bedrock and minor amount of soil, weathered N-MORB-like basaltic tholeiite, volume density = 1.15–1.20 g cm^{-3} from impact loading	XRF, redox expt., TV imaging,[d,e] impact load
Vega 1	8.10	175.85	−0.1 ± 0.1	Rusalka Planitia, N. of Aphrodite Terra, No TV panoramas, MORB-like tholeiite	γ-ray, (XRF failed)
Vega 2	−7.14	177.67	1.2 ± 0.2	Transitional zone between Rusalka Planitia and E. edge of Aphrodite Terra rise, No TV panoramas, N-MORB-like basaltic tholeiite	γ-ray, XRF

After Fegley *et al.* (1997) (reproduced by permission of the University of Arizona Press from *Venus II* **1997**, Table III).
[a] Typical uncertainties on latitude and longitude are ±1.5° (Basilevsky *et al.*, 1992). [b] Relative to modal radius of 6,051.4 km with one standard deviation uncertainties. [c] Suggested rock types are taken from Kargel *et al.* (1993) and references therein. [d] Black and white TV image for *Venera 9 and 10*; Red-green-blue TV imaging for *Venera 13 and 14*. [e] See Florensky *et al.* (1983); Garvin *et al.* (1984), and Pieters *et al.* (1986) for interpretations of the CONTRAST redox experiment, photometric data, and imaging.

potassium, uranium, and thorium by γ-ray spectroscopy, and the *Venera 13*, *14*, and *Vega 2* probes analyzed silicon, titanium, aluminum, iron, manganese, magnesium, calcium, potassium, sulfur, and chlorine by XRF spectroscopy. The γ-ray and XRF analyses are summarized in Tables 6 and 7, and are taken from Surkov *et al*. (1984, 1986, 1987).

The samples analyzed were small drill cores ~1 cm^3 from ~3 cm depth, and are probably mixtures of rock and soil, as indicated by the volume density measurements made by *Venera 13* and *14*. Elements lighter than magnesium could not be detected by XRF, and the sodium content was estimated using geochemical methods. At least some of the sulfur and chlorine in the XRF analyses could be due to atmospheric weathering instead of being primary. It is unlikely that the concentrations of any of the other elements were affected by weathering. The oxidation state of iron is not determined by XRF spectroscopy and the amounts of ferrous (Fe^{2+}) and ferric (Fe^{3+}) iron in the samples are unknown. The CONTRAST oxidation state experiments on the *Venera 13* and *14* landers gave lower limits of 0.6–7 ppmv for CO, which overlap the magnetite–hematite phase boundary at the two landing sites. Thus, both ferrous and ferric iron may be present on the surface. The imaging carried out by *Venera 13* and *14* supports this conclusion.

Several groups have performed comparisons with elemental analyses of terrestrial rocks, calculated normative mineralogical compositions, made geochemical correlations, and made geological interpretations of Magellan radar images of the *Venera* and *Vega* landing sites. Unique conclusions about the rocks present at the different landing sites are not possible, but some conclusions are broadly accepted. The *Venera 8* K/U data showed that Venus is differentiated. This ratio is higher than that for most terrestrial basalts and is closer to that for high-potassium alkaline basalts. Some authors think the *Venera 8* K/U data indicate rhyolites on Venus, but this is hard to understand on such a dry planet. The K/U ratios at the *Venera 9* and *10* landing sites are similar to those for terrestrial alkaline basalts and oceanic tholeiites. The *Venera 13* XRF analysis suggests high-potassium alkaline basalts. The rocks at the *Venera 8* and *Venera 13* sites are generally thought to be similar, but this is not certain. The *Venera 14* XRF analysis suggests rocks like normal mid-ocean ridge basalt (N-MORB) that have been

Table 6 XRF elemental analyses of Venus' surface.

Oxide	*Mass percent*[a]				
	Venera 13[b]	*Leucitic basalt*[c]	*Venera 14*[b]	*Vega 2*[d,e]	*N-MORB*[f]
SiO_2	45.1 ± 3.0	46.18	48.7 ± 3.6	45.6 ± 3.2	48.77
TiO_2	1.59 ± 0.45	2.13	1.25 ± 0.41	0.2 ± 0.1	1.15
Al_2O_3	15.8 ± 3.0	12.74	17.9 ± 2.6	16 ± 1.8	15.9
FeO[g]	9.3 ± 2.2	9.86	8.8 ± 1.8	7.7 ± 1.1	9.82
MnO	0.2 ± 0.1	0.19	0.16 ± 0.08	0.14 ± 0.12	0.17
MgO	11.4 ± 6.2	8.36	8.1 ± 3.3	11.5 ± 3.7	9.67
CaO	7.1 ± 0.96	8.16	10.3 ± 1.2	7.5 ± 0.7	11.16
Na_2O[h]	2 ± 0.5	2.36	2.4 ± 0.4	2.0	2.43
K_2O	4.0 ± 0.63	6.18	0.2 ± 0.07	0.1 ± 0.08	0.08
SO_3	1.62 ± 1.0	0.09	0.88 ± 0.77	4.7 ± 1.5	
Cl	<0.3		<0.4	<0.3	
Total	98.1	96.16	98.7	95.4	99.15

[a] Error values for *Venera 13, 14*, and *Vega 2* data are ±1σ. [b] Surkov *et al.* (1984). [c] Volkov *et al.* (1986). [d] Surkov *et al.* (1986). [e] In addition to Cl, Surkov *et al.* (1986) also report the following upper limits (in mass %): Cu, Pb < 0.3; Zn < 0.2; Sr, Y, Zr, Nb, Mo < 0.1; As, Se, Br < 0.08. [f] Wilson (1989). [g] All Fe reported as FeO for all analyses. [h] Calculated by Surkov *et al.* (1984, 1986).

Table 7 Gamma ray analyses of Venus' surface.

Space probe	*K* (%)	*U* (ppm)	*Th* (ppm)	*K/U ratio*
Venera 8	4.0 ± 1.2	2.2 ± 0.7	6.5 ± 2.2	$18{,}200^{+16{,}500}_{-8{,}500}$
Venera 9	0.47 ± 0.08	0.60 ± 0.16	3.65 ± 0.42	$7{,}800^{+4{,}700}_{-2{,}700}$
Venera 10	0.30 ± 0.16	0.46 ± 0.26	0.70 ± 0.34	$6{,}500^{+16{,}500}_{-4{,}600}$
Vega 1	0.45 ± 0.22	0.64 ± 0.47	1.5 ± 1.2	$7{,}000^{+32{,}400}_{-4{,}900}$
Vega 2	0.40 ± 0.20	0.68 ± 0.38	2.0 ± 1.0	$5{,}900^{+14{,}100}_{-4{,}000}$

Source: Surkov *et al.* (1987).

weathered by atmospheric SO_2. The *Vega 1* XRF spectrometer failed and only γ-ray data are available. The K/U ratios are similar to those at the *Venera 9* and *10* sites. The *Vega 2* XRF and γ-ray data suggest rocks like those at the *Venera 14* site, namely, weathered N-MORB-like basalts. The difference between the potassium content determined by the XRF and γ-ray instruments may reflect a difference between two different analyzed samples. The high sulfur contents in the three XRF analyses may be due to chemical weathering by atmospheric SO_2 to form anhydrite ($CaSO_4$) or sulfate-bearing scapolite. Conversely, the sulfur could be primary anhydrite or iron sulfide as in some terrestrial lavas (Carroll and Rutherford, 1985).

Normative compositions for the *Venera 13*, *14*, and *Vega 2* XRF analyses are given in Table 8, along with comparisons to the norms for terrestrial rocks that are possible analogues to the samples analyzed on Venus. Sulfur and chlorine were excluded from the norms in Table 8. If all sulfur is assumed present as anhydrite, then anhydrite comprises 2.8 ± 1.7 mass%, 1.5 ± 1.3 mass%, and 8.2 ± 2.6 mass%, of the *Venera 13*, *14*, and *Vega 2* samples, respectively. Table 8 also shows that calculated liquidus temperatures for the Venusian samples are similar to the liquidus temperatures of the possible terrestrial analogues.

1.19.4.2 Atmosphere–Surface Interactions

The high temperatures and pressures drive chemical reactions of CO_2, SO_2, OCS, H_2S, HCl, and HF with rocks and minerals on Venus' surface. A possible exception is sulfur vapor chemistry initiated by absorption of blue sunlight. After the *Mariner 2* flyby Mueller (1963) wrote that Venus' surface temperature "corresponds with those [temperatures] attained during moderately high degrees of metamorphism on Earth. It is therefore possible that large parts of the atmosphere of Venus are partially equilibrated with the surface rocks. From this assumption, it follows that the composition of the atmosphere should reflect the mineralogical character of the rocks." However, as of early 2003, Mueller's assumption remains controversial and unproven.

During the 1960s and 1970s Mueller and J. S. Lewis in the US, and scientists with the Soviet Venus exploration program modeled thermochemical equilibria between gases and minerals expected on Venus' surface. The models predicted that the abundances of CO_2, SO_2, OCS, H_2O, HCl, and HF are controlled by reactions with reactive minerals on Venus' surface. From today's perspective it now seems that only the abundances of CO_2, HCl, and HF are regulated, or buffered by the surface mineralogy, while the abundances of water vapor, CO, and the sulfur gases are kinetically controlled by combinations of surface–atmosphere reactions and gas-phase chemistry.

1.19.4.2.1 Carbonate equilibria

The CO_2 pressure on Venus is plausibly regulated by the "Urey reaction,"

$$CaCO_3(\text{calcite}) + SiO_2(\text{silica}) = CaSiO_3(\text{wollastonite}) + CO_2 \quad (12)$$

$$\log_{10} P_{CO_2} = 7.97 - 4,456/T \quad (13)$$

because the CO_2 pressure of ~92 bar at 740 K is virtually identical to the equilibrium CO_2 pressure from reaction (12) at that temperature (Fegley and Treiman, 1992). But, are carbonates present on Venus?

Arguments in favor of carbonates include the following. Some of the flow features on Venus' surface look like they were made by magmas, such as carbonatites, with water-like rheologies. If correct, these geomorphological interpretations

Table 8 Normative compositions of Venusian samples and possible terrestrial analogues.

CIPW norms	*Venera 13*[a]	*Leucitic basalt*[a]	*Venera 14*[a]	*Tholeiitic basalt*[a]	*Vega 2*[b]
Hypersthene			18.2	14.2	25.4
Olivine	26.6	16.6	9.1	8.1	13.9
Diopside	10.2	29.4	9.9	21.2	2.5[d]
Anorthite	24.2	6.2	38.6	33.6	38.3
Albite	3.0		20.7	20.3	18.9
Orthoclase	25.0	11.8	1.2	0.3	0.5
Nepheline	8.0	11.2			
Leucite		20.6			
Ilmenite	3.0	4.2	2.3	2.3	0.5
Total	100.0	100.0	100.0	100.0	100.0
Liquidus T (°C)[c]	1,249	1,176	1,153	1,196	1,265

[a] On a volatile free basis, from Volkov *et al.* (1986). [b] Barsukov *et al.* (1986). [c] Liquidus temperatures calculated with the MAGPOX3 code of John Longhi. [d] Clinopyroxene.

mean that carbonates are present on Venus. Also, as done with the Viking XRF analyses, the mass deficits in the *Venera* and *Vega* XRF analyses can be attributed to carbonates. The calculated calcite abundances (by mass) are 4% at the *Venera 13* site, 3% at the *Venera 14* site, and 10% at the *Vega 2* site. Carbonate-bearing rocks would also provide chlorine- and fluorine-bearing minerals necessary for regulating the atmospheric abundances of the reactive hydrogen halides.

There are two major arguments against carbonates. Most terrestrial carbonates are sedimentary, while Venus is dry without liquid water. However, the high D/H ratio suggests that Venus was wet in the past and carbonates may have formed at that time. Second, calculations and experiments predict that carbonates on Venus will react with atmospheric SO_2 to form anhydrite ($CaSO_4$). However, the *Venera* XRF analyses show CaO/SO_3 ratios less than unity, so Venus' surface is not anhydrite saturated. Also, wind-driven erosion may abrade anhydrite layers and expose the underlying carbonate. But at present the questions of whether or not carbonates are present on Venus and are buffering atmospheric CO_2 remain unresolved. Sample return or *in situ* analyses that are sensitive to calcite and other carbonates are needed to answer these questions.

1.19.4.2.2 Equilibria involving HCl and HF

Hydrogen chloride and HF were discovered in Venus' atmosphere in the late 1960s. Shortly thereafter, it was proposed that the atmospheric abundances HCl and HF are regulated by equilibria involving chlorine- and fluorine-bearing minerals, such as sodalite or fluorphlogopite. For example, a reaction involving nepheline, albite, and sodalite

$$\begin{aligned} &2HCl(g) + 9NaAlSiO_4(\text{nepheline}) \\ &\quad = Al_2O_3(\text{corundum}) + NaAlSi_3O_8(\text{albite}) \\ &\qquad + 2Na_4[AlSiO_4]_3Cl(\text{sodalite}) \\ &\qquad + H_2O(g) \end{aligned} \tag{14}$$

may buffer HCl, while a reaction involving potassium feldspar and fluorphlogopite

$$\begin{aligned} &2HF(g) + KAlSi_3O_8(\text{K-spar}) \\ &\quad + 3MgSiO_3(\text{enstatite}) \\ &\qquad = KMg_3AlSi_3O_{10}F_2(\text{fluorphlogopite}) \\ &\qquad\quad + 3SiO_2(\text{silica}) + H_2O(g) \end{aligned} \tag{15}$$

may buffer HF (Fegley *et al.*, 1997). These reactions as well as other possible buffers for HCl and HF involve phases that are common in alkaline rocks on Earth and by analogy also on Venus. This is an interesting point because alkaline rocks, which are rare on Earth, seem to be present at several of the *Venera* and *Vega* landing sites. As argued by Kargel *et al.* (1993), Venus may have a more mafic alkaline crust than the Earth.

1.19.4.2.3 Redox reactions involving iron-bearing minerals

The oxidation of Fe^{2+}-bearing minerals in basalt (and other volcanic rocks on Venus' surface) is potentially very important for water loss via oxidation of the surface and hydrogen escape to space. The overall process is schematically represented by

$$\begin{aligned} &H_2O(\text{gas}) + 2FeO(\text{in rock}) \\ &\quad = Fe_2O_3(\text{hematite}) + H_2(\text{gas}) \end{aligned} \tag{16}$$

and

$$\begin{aligned} &H_2O(\text{gas}) + 3FeO(\text{in rock}) \\ &\quad = Fe_3O_4(\text{magnetite}) + H_2(\text{gas}) \end{aligned} \tag{17}$$

where FeO represents the Fe^{2+}-bearing pyroxenes, olivines, etc., in a rock. Several spacecraft observations indicate that oxidation of Fe^{2+}-bearing basalts occurs on Venus today. Wide-angle photometry at the *Venera 9* and *10* sites and color TV imaging at the *Venera 13* and *14* sites suggest the presence of hematite or another ferric iron mineral on Venus' surface (Pieters *et al.*, 1986). The electrical resistivity of the soil at the *Venera 13* and *14* landing sites was measured and found to be one to two orders of magnitude lower than for basalt at the same temperature. Electrically conductive minerals such as magnetite and/or hematite may be present. As noted above, the CONTRAST oxidation state experiments on these landers gave lower limits of 0.6–7 ppmv for CO, which overlap the magnetite–hematite phase boundary. The PV large probe neutral mass spectrometer reported 0–10 ppmv H_2 below 25 km. The PV Orbiter ion mass spectrometer detected a mass-2 peak that has been interpreted in terms of contributions from D^+ and H_2^+ (Donahue *et al.*, 1997). The derived H_2 mixing ratio is $<$0.1–10 ppmv below 140 km altitude. The *Venera 13 and 14* GC reported 25 $\pm$ 10 ppmv H_2 at 49–58 km (Krasnopolsky, 1986). The latter detection is controversial. In any case, the reported H_2 mixing ratio in Venus' lower atmosphere ranges from $<$0.1 ppmv to 10–25 ppmv. These H_2 mixing ratios are larger than those from the water–gas reaction

$$CO + H_2O = CO_2 + H_2 \tag{18}$$

at Venus surface temperatures and indicate that oxidation of Fe^{2+}-bearing minerals by H_2O may be involved in producing the observed hydrogen.

1.19.4.2.4 *Minerals present in low radar emissivity regions*

Radar observations from the *Pioneer Venus* and *Magellan* spacecraft show global variations in the radar emissivity of Venus' surface (Pettengill *et al*., 1996, 1997). The variations are apparently mainly related to the types of rocks present. Typically, regions below ~2.4 km elevation (i.e., below 6,054 km radius) have radar properties characteristic of anhydrous rocks, such as dry basalt. However, higher elevation regions have lower radar emissivity, indicating the presence of semiconducting minerals with high dielectric constants. The critical level also shifts upward by ~1 km from the equator to high northern latitudes. The sharp boundary between normal rock at lower elevations and lower-emissivity rock at higher elevations indicates that temperature changes play a role in the unusual chemistry.

Several proposals have been made for the chemistry and minerals involved. The loaded dielectric model uses inclusions of iron sulfides, or other high dielectric minerals, in rocks. Higher amounts of the dielectric minerals produce lower radar emissivities and higher dielectric constants. The iron sulfides, or other dielectric minerals, are destroyed by chemical reactions with Venus' atmosphere. The reactions proceed faster at lower elevations, where the temperatures are higher, so the lowest radar emissivity regions are predicted at the highest elevations, or in areas with the youngest volcanic rocks.

The metallic frost model postulates volcanic outgassing and condensation of volatile elements and their compounds, such as elemental tellurium or galena (PbS), on mountain tops and other high-elevation areas. Many volatile elements (e.g., copper, zinc, tin, lead, arsenic, antimony, and bismuth) form halides or chalcogenides with high vapor pressures. Compounds of these metals are typically found around terrestrial volcanic vents and fumaroles, or are present in volcanic gases (Brackett *et al*., 1995). Many of these elements and their compounds are semiconductors and have high dielectric constants. Volcanic eruptions release these volatile elements and their compounds, which then condense as metallic frosts on Venus' surface. The metallic frosts concentrate in the higher-elevation regions, which are cold traps for them (Brackett *et al*., 1995), like snow on Mount Kilimanjaro. Thin layers of such metallic frosts can account for the observed radar properties, e.g., a 5 μm thick layer of elemental tellurium (Pettengill *et al*., 1996). The metallic frost layers can be covered and/or vaporized by fresh volcanic flows, which should display normal radar emissivity. The radar properties do not uniquely constrain the semiconductor(s) present, which will remain unknown until elemental and mineralogical analyses are carried out *in situ* or on samples returned from low-emissivity highlands regions.

1.19.4.3 The Venus Sulfur Cycle and Climate Change

Current knowledge suggests that volcanic outgassing on Venus produces SO_2 and the reduced sulfur gases S_2, OCS, and H_2S. The relative proportions of these species in Venusian volcanic gases are unknown. Sulfur dioxide is generally the major sulfur gas in terrestrial basaltic volcanic gases, which have oxygen fugacities between those of the quartz–fayalite–magnetite (QFM) and nickel–nickel oxide (NNO) buffers (Symonds *et al*., 1994). Hydrogen sulfide is often the next most abundant sulfur gas, and is sometimes as or more abundant than SO_2. Carbonyl sulfide and sulfur vapor are less abundant than SO_2 or H_2S. If Venusian basalts erupt at temperatures and oxygen fugacities similar to those for terrestrial basaltic volcanoes, then SO_2 should be more abundant than S_2, OCS, or H_2S. The very low H_2O abundance in Venus' atmosphere and considerations of chemical equilibria also imply that S_2 and OCS should be more abundant than H_2S in Venusian volcanic gases.

At present, the SO_2 abundance in Venus' atmosphere is 35–110 times larger than the equilibrium SO_2 pressure for the reaction

$$SO_2 + CaCO_3(\text{calcite}) = CaSO_4(\text{anhydrite}) + CO \qquad (19)$$

which is thus a sink for SO_2. The *Vega* UV spectrometer data give the lower factor of 35, while *Pioneer Venus*, *Venera 11–12*, and Earth-based IR spectroscopic data give the higher factor of 110 (cf. Fegley *et al*., 1997, figure 7). The rate of reaction (19) is known and it is sufficient to remove all SO_2 (and thus the sulfuric acid clouds) from Venus' atmosphere in ~1.9 Myr in the absence of a volcanic source (Fegley and Prinn, 1989). Similar, but slower, reactions of SO_2 occur with other calcium-bearing minerals such as anorthite, diopside, and wollastonite. The measured Ca/S ratios are greater than unity at the *Venera 13*, *14*, and *Vega 2* sites. These ratios are larger than expected (i.e., unity) if all calcium were combined with sulfur in anhydrite. Thus, loss of atmospheric SO_2 via chemical weathering of calcium-bearing minerals on Venus' surface is probably an ongoing process.

Maintenance of atmospheric SO_2 at its current concentration requires eruption of ~1 km^3 yr of lava with the average composition of the *Venera 13*, *14*, and *Vega 2* landing sites.

This volcanism rate is the same as the average rate of subaerial volcanism on Earth and is ~5% of the terrestrial plate creation rate of ~20 $km^3\ yr^{-1}$. The required sulfur eruption rate to maintain SO_2 on Venus at steady state is ~28 $Tg\ yr^{-1}$. This is similar to estimates of 9 (subaerial), 19 (submarine), and 28 (total) $Tg\ yr^{-1}$ for SO_2 emissions from terrestrial volcanism (Charlson *et al.*, 1992).

Volcanism on Earth and on Io is episodic. By analogy, Venusian volcanism should be episodic, which may be one reason why active volcanism has not yet been seen on Venus. However, a volcanic source for SO_2 is required at present. What may happen if the volcanic source and anhydrite sink for SO_2 are not balanced? If less SO_2 is erupted than is lost by anhydrite formation, less SO_2 will be left in the atmosphere, less H_2SO_4 will be produced, and fewer clouds will form. Temperatures in Venus' atmosphere and at the surface may decrease, because SO_2 and volcanic volatiles such as CO_2 and H_2O are greenhouse gases. Magnesite ($MgCO_3$) and other carbonates unstable on Venus today may form and consume atmospheric CO_2 as temperatures drop. Conversely, if more SO_2 is erupted than is lost by anhydrite formation, more SO_2 will be added to the atmosphere, more H_2SO_4 will be produced, and more clouds will form. In this case atmospheric and surface temperatures may rise as more greenhouse gases enter the atmosphere. Minerals now stable at 740 K on Venus' surface may decompose as temperatures increase.

Some of these effects, which could operate in the future and may have done so in the past, have been studied in climate models that incorporate variations of SO_2 and H_2O abundances on the clouds and temperatures on Venus (e.g., Hashimoto and Abe, 2001; Bullock and Grinspoon, 2001). In particular, large temperature changes are predicted to result from the putative global resurfacing of Venus 500 ± 200 Ma. Solomon *et al.* (1999) modeled the atmospheric and geophysical consequences of this event. They propose that higher surface temperatures diffuse into Venus' interior and cause significant thermal stresses that influence tectonic deformation on a global scale. Their model may explain formation of some of the wrinkled ridge plains that cover 60–65% of Venus' surface today.

Finally, the role of OCS and H_2S in the Venus sulfur cycle needs to be considered. In addition to their possible volcanic sources, chemical weathering of iron sulfides may produce OCS and H_2S. These sources are exemplified by the following reactions:

$$4CO_2 + 3FeS(\text{pyrrhotite}) = 3OCS + CO + Fe_3O_4(\text{magnetite}) \quad (20)$$

$$4H_2O + 3FeS(\text{pyrrhotite}) = 3H_2S + H_2 + Fe_3O_4(\text{magnetite}) \quad (21)$$

The inferred gradient in OCS and observation by the *Pioneer Venus* mass spectrometer of 3 ± 2 ppmv H_2S below 22 km are consistent with these ideas. At higher altitudes, OCS and H_2S are converted to SO_2 via photochemical reactions that result in the net transformations:

$$2H_2S + 6CO_2 \rightarrow 2H_2O + 2SO_2 + 6CO \quad (22)$$

$$2OCS + 4CO_2 \rightarrow 2SO_2 + 6CO \quad (23)$$

The SO_2 is then photo-oxidized to aqueous sulfuric acid droplets as described earlier.

The sulfur cycle is closed as follows. Sulfuric acid cloud droplets vaporize to a gas mixture of H_2SO_4, SO_3, and H_2O at the cloud base. Reduction of SO_3 to SO_2 occurs via the reaction

$$CO + SO_3 \rightarrow SO_2 + CO_2 \quad (24)$$

The SO_2 formed via reaction (24) eventually reacts with calcium-bearing minerals on Venus's surface and the cycle repeats when sulfur gases are volcanically outgassed again.

1.19.4.4 Topography and Geology

Venus is often regarded as Earth's "twin planet" because of its similar size (~95%), mass (~82%), and gravity (~90%) compared to Earth. However, radar images from Earth-based observatories and from the *Pioneer Venus*, *Venera 15/16*, and *Magellan* spacecraft reveal both important similarities and differences to the Earth. Tanaka *et al.* (1997) distinguish three major terrain types on Venus: (i) lowlands, which comprise ~27% of Venus' surface that lies ~0–2 km below the modal radius (6,051.4 km); (ii) upland rolling plains, which comprise ~65% of the surface at an elevation of ~0–2 km; and (iii) highlands that are ~8% of the surface and are >2 km above the modal radius. The total range of elevations on Venus is ~14 km from Diana Chasma (−2 km) to the top of Maxwell Montes (12 km). However, ~80% of the surface is within ±1 km, and ~90% is between −1 km and +2.5 km of the modal radius. Venus' unimodal topographic distribution is in contrast to Earth, which has a bimodal hypsometric curve. Figure 2 shows the hypsometric curve for Venus.

The two major highland regions on Venus are Ishtar Terra at high northern latitudes and Aphrodite Terra in the equatorial regions. Both regions are continental in size. Ishtar is about the same size as Australia, while Aphrodite is roughly the size of South America. The western part of Ishtar is dominated by the Lakshmi Planum plateau that resembles, but is larger

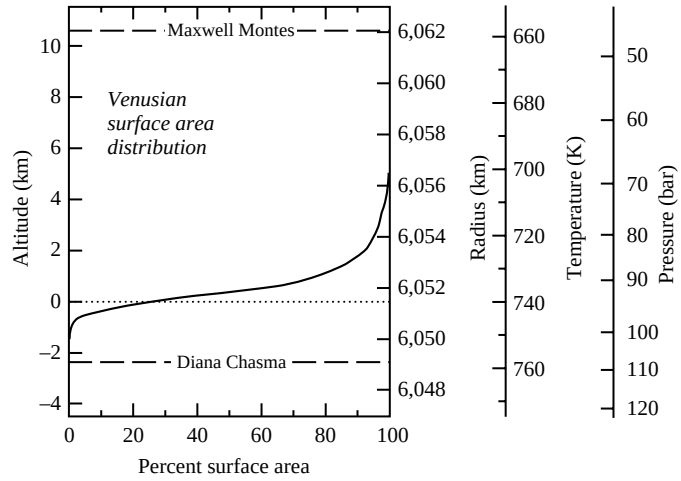

Figure 2 Distribution of surface area as a function of altitude for Venus, i.e., the hypsometric curve (after Fegley and Treiman, 1992) (reproduced by permission of American Geophysical Union from *Geophysical Monograph* **1992**, 66).

than, the Tibetan plateau on Earth. Maxwell Montes, which is higher than Mount Everest, is in eastern Ishtar. Aphrodite is rougher and more complex than Ishtar and is characterized by several deep narrow valleys, such as Diana Chasma, and by several distinct mountain ranges that reach up to 6 km high. Alpha, Beta, and Phoebe Regio are three smaller highland regions.

Venus' surface shows extensive evidence of widespread volcanism including large shield volcanoes such as Sif Mons, that are similar to the shield volcanoes of the Hawaiian islands, volcanic plains, volcanic calderas, smaller volcanic landforms such as cones and pancake domes, and long sinuous channels (such as Baltis Vallis) that can meander for several thousand kilometers across the surface. In some cases, the different landforms indicate different types of magmas, for example, the pancake domes were apparently formed by viscous SiO_2-rich magmas, whereas the long sinuous channels were apparently formed by fluid magmas, such as carbonatites or even liquid sulfur.

Tectonic features are also present on the surface. Tesserae, which are tectonically deformed regions formed by piling up blocks of crust, are common in the highlands. As noted earlier, ~65% of Venus' surface is covered by tectonically deformed lowlands and rolling plains containing wrinkle ridges formed by buckling of the crust. Other features formed by volcanism and tectonism are coronae, circular- or oval-shaped features a few hundred kilometers in diameter that may have raised outer rims and arachnoids, which are caldera-like collapse features surrounded by fractures. The topography of coronae is highly variable. Most of the coronae occur in chains associated with large scale rifting (chasmata), some occur in association with volcanic rises, and a few are isolated features in the plains.

Venus' surface has ~940 impact craters ranging in diameter from ~3 km to a few hundred kilometers. The small size cutoff is probably due to atmospheric disruption of small impactors. The smaller craters are more irregularly shaped, indicating the impact of several fragments instead of one object. The crater ejecta patterns are unlike those on other solar system bodies and probably have been affected by the dense atmosphere and prevailing winds. The number and distribution of craters was used to argue for global volcanism resurfacing ~500 ± 200 Ma (Schaber *et al.*, 1992). However, this interpretation has been questioned by other workers, who argue that two large-scale plain units of distinct ages spread over 400 Ma exist instead (Hauck *et al.*, 1998).

1.19.4.5 Interior

Venus' interior structure is unknown, but spacecraft data allow several inferences. No intrinsic magnetic field has been detected, and any dipole field is $<10^{-4}$ that of Earth. The ~243 d rotation rate may be too slow to generate a field by dynamo action in a core. Radar imaging does not show evidence of plate tectonics, which may be due to a lack of water and/or to difficulty in subducting the lithosphere, which is hotter and perhaps more buoyant than on Earth because of Venus' high surface temperature. The *Magellan* gravity data provide the best probe of Venus' interior. Unlike Earth, gravity is strongly correlated with topography on Venus, suggesting that higher regions are above regions of mantle upwelling. Figure 3 is a cartoon illustrating Venus' internal

structure. Three models of Venus' (unknown) bulk composition are given in Table 9. The chondritic meteorite model assumes that the processes that affected chondritic meteorites in the solar nebula also affected the material accreted by terrestrial planets. Planetary bulk compositions are predicted based on abundances of key elements such as potassium and uranium that have been determined by sample return or *in situ* analyses. The equilibrium condensation model predicts planetary compositions based on temperature- and pressure-dependent thermodynamic equilibrium in a solar nebula model with T and P known as a function of radial distance. The pyrolite model is similar to the pyrolite model for the Earth and uses analyses of basalts and geochemical constraints to predict planetary compositions.

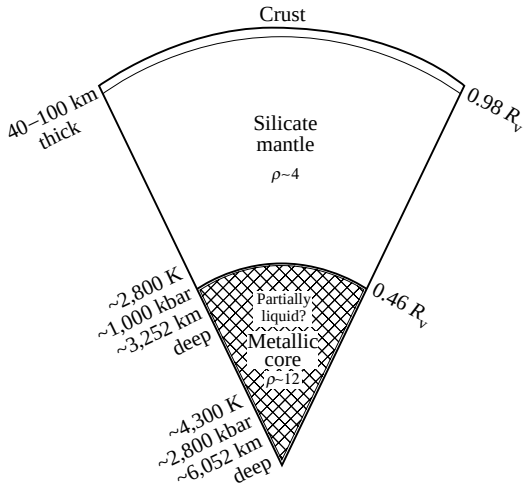

Figure 3 A cartoon illustrating Venus' interior structure based on current bulk composition models (see Table 9) (after Lodders and Fegley, 1998) (reproduced by permission of Oxford University Press from the *Planetary Scientist's Companion* **1998**, p. 118).

Table 9 Bulk composition models for Venus.

Component	*Chondritic meteorite*[a]	*Equilibrium condensation*[b]	*Pyrolite*[c]
Mantle/Crust			
SiO_2	49.8	52.9	40.4
TiO_2	0.21	0.20	0.24
Al_2O_3	4.1	3.8	3.4
FeO	5.4	0.24	18.7
Cr_2O_3	0.87		0.3
MnO	0.09		0.2
MgO	35.5	37.6	33.3
CaO	3.3	3.6	3.4
Na_2O	0.28	1.6	0.15
K_2O	0.027	0.174	0.018
Core			
Fe	88.6	94.4	78.7
Ni	5.5	5.6	6.6
Co	0.26		
S	5.1	0	4.9
O	0		9.8
Mass fractions			
Core	0.32	0.30	0.24
Mantle + Crust	0.68	0.70	0.76

After Lodders and Fegley (1998).
[a] Morgan and Anders (1980). [b] Basaltic Volcanism Study Project model Ve1. [c] BVSP model Ve4.

1.19.5 SUMMARY OF KEY QUESTIONS

Some of the key questions about Venus that are unresolved include the following. What is the oxygen isotopic composition (all three stable isotopes) of the silicate portion of Venus? Oxygen is either the first or second most abundant element in Venus, and its isotopic composition can help constrain accretion models for the terrestrial planets. The Earth and Moon have the same oxygen isotopic composition, but the oxygen isotopic composition of the SNC meteorite parent body, presumably Mars, of the eucrite parent body, presumably 4 Vesta, and of other meteorites, and IDPs are different. It is important to measure abundances of the three oxygen isotopes (with an uncertainty of $<0.1‰$) on Venus to see if it has the same or a different oxygen isotopic composition as the Earth and Moon. These measurements would have to be carried out on samples returned from Venus, which is technologically feasible at present.

Another important question is which, if any, gases in Venus' atmosphere are buffered by mineral assemblages on Venus' surface. Interpretations of data from *Pioneer Venus* and the *Venera* and *Vega* probes about the chemistry of Venus' lower atmosphere and surface are based upon this assumption, which has not been verified experimentally. Instead, research shows kinetic control of reactions of SO_2 and water vapor with minerals at Venus surface temperatures (Fegley and Prinn, 1989; Johnson and Fegley, 2000).

Finally, it is also important to understand the origin, duration, and stability of the Venusian super-greenhouse. The Venus sulfur cycle demonstrates the close connection between chemistry and climate on Venus, because SO_2 is one of the three key greenhouse gases sustaining the super-greenhouse, is involved in chemical reactions with abundant calcium-bearing minerals on the surface, is the feedstock for the global sulfuric acid clouds, and is probably also an important volcanic volatile. Current knowledge of the super-greenhouse and of climate change and stability on Venus requires new laboratory studies of IR absorption bands in hot, dense CO_2, SO_2, and H_2O and improved computer models of the influence of clouds on climate.

ACKNOWLEDGMENTS

I thank K. Baines, B. Bézard, D. Cahn, D. Crisp, A. Davis, K. Lodders, V. Moroz, R. Pepin, R. Wieler for discussions and R. Osborne for assistance with preparing the manuscript. This work was supported by Grant NAG5-11037 from the NASA Planetary Atmospheres Program.

REFERENCES

Allen D. A. and Crawford J. W. (1984) Cloud structure on the dark side of Venus. *Nature* **307**, 222–224.

Baines K. H. and 24 others (2000) Detection of sub-micron radiation from the surface of Venus by Cassini/VIMS. *Icarus* **148**, 307–311.

Barath F. T., Barrett A. H., Copeland J., Jones D. E., and Lilley A. E. (1964) Mariner 2 microwave radiometer experiment and results. *Astron. J.* **69**, 49–58.

Barker E. S. (1979) Detection of SO_2 in the UV spectrum of Venus. *Geophys. Res. Lett.* **6**, 117–120.

Barsukov V. L., Surkov Yu. A., Dmitriyev L. V., and Khodakovsky I. L. (1986) Geochemical studies on Venus with the landers from the Vega-1 and Vega-2 probes. *Geochem. Int.* **23**(7), 53–65.

Barsukov V. L., Basilevsky A. T., Volkov V. P., and Zharkov V. N. (eds.) (1992) *Venus Geology, Geochemistry, and Geophysics.* University of Arizona Press, Tucson.

Basilevsky A. T., Nikolaeva O. V., and Weitz C. M. (1992) Geology of the Venera 8 landing site region from Magellan data: morphological and geochemical considerations. *J. Geophys. Res.* **97**, 16315–16335.

Bézard B., Baluteau J. P., Marten A., and Coron N. (1987) The $^{12}C/^{13}C$ and $^{16}O/^{18}O$ ratios in the atmosphere on Venus from high-resolution 10-μm spectroscopy. *Icarus* **72**, 623–634.

Bézard B., DeBergh C., Crisp D., and Maillard J. P. (1990) The deep atmosphere of Venus revealed by high-resolution nightside spectra. *Nature* **345**, 508–511.

Bougher S. W., Hunten D. M., and Phillips R. J. (eds.) (1997) *Venus II*. University of Arizona Press, Tucson, 1362pp.

Brackett R. A., Fegley B., Jr., and Arvidson R. E. (1995) Volatile transport on Venus and implications for surface geochemistry and geology. *J. Geophys. Res.* **100**, 1553–1563.

Bullock M. A. and Grinspoon D. H. (2001) The recent evolution of climate on Venus. *Icarus* **150**, 19–37.

Carroll M. R. and Rutherford J. J. (1985) Sulfide and sulfate saturation in hydrous silicate melts. *Proc. 15th Lunar Planet Sci. Conf. J. Geophys. Res. Suppl.* **90**, C601–C612.

Chamberlain J. W. and Hunten D. M. (1987) *Theory of Planetary Atmospheres*. Academic Press, San Diego.

Charlson R. J., Anderson T. L., and McDuff R. E. (1992) The sulfur cycle. In *Global Biogeochemical Cycles* (eds. S. S. Butcher, R. J. Charlson, G. H. Orians, and G. V. Wolfe). Academic Press, London, pp. 285–300.

Connes P., Connes J., Benedict W. S., and Kaplan L. D. (1967) Traces of HCl and HF in the atmosphere of Venus. *Astrophys. J.* **147**, 1230–1237.

Connes P., Connes J., Kaplan L. D., and Benedict W. S. (1968) Carbon monoxide in the Venus atmosphere. *Astrophys. J.* **152**, 731–743.

Crisp D. and Titov D. (1997) The thermal balance of the Venus atmosphere. In *Venus II* (eds. S. W. Bougher, D. M. Hunten, and R. J. Phillips). University of Arizona Press, Tucson, pp. 353–384.

Donahue T. M., Grinspoon D. H., Hartle R. E., and Hodges R. R., Jr. (1997) Ion/neutral escape of hydrogen and deuterium: evolution of water. In *Venus II* (eds. S. W. Bougher, D. M. Hunten, and R. J. Phillips). University of Arizona Press, Tucson, pp. 385–414.

Esposito L. W., Knollenberg R. G., Marov M. Ya., Toon O. B., and Turco R. P. (1983) The clouds and hazes of Venus. In *Venus* (eds. D. M. Hunten, L. Colin, T. M. Donahue, and V. I. Moroz). University of Arizona Press, Tucson, pp. 484–564.

Esposito L. W., Burtaux J.-L., Krasnopolsky V., Moroz V. I., and Zasova L. V. (1997) Chemistry of the lower atmosphere and clouds. In *Venus II* (eds. S. W. Bougher, D. M. Hunter, and R. J. Phillips). University of Arizona Press, Tucson, pp. 415–458.

Fegley B., Jr. and Prinn R. G. (1989) Estimation of the rate of volcanism on Venus from reaction rate measurements. *Nature* **337**, 55–58.

Fegley B. and Treiman A. H. (1992) Chemistry of atmosphere-surface interactions on Venus and Mars. In *Venus and Mars: Atmospheres, Ionospheres, and Solar Wind Interactions*, Geophysical Monograph 66 (eds. J. G. Luhmann, M. Tatrallyay, and R. O. Pepin). American Geophysical Union, Washington, DC, pp. 7–71.

Fegley B., Jr., Klingelhöfer G., Lodders K., and Widemann T. (1997) Geochemistry of surface-atmosphere interactions on Venus. In *Venus II* (eds. S. W. Bougher, D. M. Hunten, and R. J. Phillips). University of Arizona Press, Tucson, pp. 591–636.

Florensky C. P., Nikolaeva O. V., Volkov V. P., Kudryashova A. F., Pronin A. A., Geektin Yu. M., Tchaikina E. A., and Bashkirova A. S. (1983) Redox indicator "CONTRAST" on the surface of Venus. *Lunar Planet. Sci.* **XIV**. (abstract). The Lunar and Planetary Institute, Houston, pp. 203–204.

Fox J. L. and Kliore A. J. (1997) Ionosphere: solar cycle variations. In *Venus II* (eds. S. W. Bougher, D. M. Hunten, and R. J. Phillips). University of Arizona Press, Tucson, pp. 161–188.

Garvin J. B., Head J. W., Zuber M. T., and Helfenstein P. (1984) Venus: the nature of the surface from Venus panoramas. *J. Geophys. Res.* **89**, 3381–3399.

Gierasch P. J., Goody R. M., Young R. E., Crisp D., Edwards C., Kahn R., Rider D., Del Genio A., Greeley R., Hou A., Leovy C. B., McCleese D., and Newman M. (1997) The general circulation of the Venus atmosphere: an assessment. In *Venus II* (eds. S. W. Bougher, D. M. Hunten, and R. J. Phillips). University of Arizona Press, pp. 459–500.

Hashimoto G. L. and Abe Y. (2001) Predictions of a simple cloud model for water vapor cloud albedo feedback on Venus. *J. Geophys. Res.* **106**, 14675–14690.

Hauck S. A., Phillips R. J., and Price M. H. (1998) Venus: crater distribution and plains resurfacing models. *J. Geophys. Res.* **103**, 13635–13642.

Hunt G. E. and Moore P. (1982) *The Planet Venus*. Faber and Faber, London.

Hunten D. M., Colin L., Donahue T. M., and Moroz V. I. (eds.) (1983) *Venus*. University of Arizona Press, Tucson.

Jastrow R. and Rasool S. I. (eds.) (1969) *The Venus Atmosphere*. Gordon and Breach, New York.

Johnson N. M. and Fegley B., Jr. (2000) Water on Venus: new insights from tremolite decomposition. *Icarus* **146**, 301–306.

Kargel J. S., Komatsu G., Baker V. R., and Strom R. G. (1993) The volcanology of Venera and VEGA landing sites and the geochemistry of Venus. *Icarus* **103**, 253–275.

Kasprzak W. T., Keating G. M., Hsu N. C., Stewart A. I. F., Colwell W. B., and Bougher S. W. (1997) Solar activity behavior of the thermosphere. In *Venus II* (eds. S. W. Bougher, D. M. Hunten, and R. J. Phillips). University of Arizona Press, Tucson, pp. 225–257.

Kaula W. M. (1999) Constraints on Venus evolution from radiogenic argon. *Icarus* **139**, 32–39.

Krasnopolsky V. A. (1986) *Photochemistry of the Atmospheres of Mars and Venus*. Springer, Berlin.

Lewis J. S. and Prinn R. G. (1984) *Planets and their Atmospheres*. Academic Press, Orlando.

Lodders K. and Fegley B., Jr. (1998) *The Planetary Scientist's Companion*. Oxford University Press, New York.

Maor E. (2000) *June 8, 2004 Venus in Transit*. Princeton University Press, Princeton.

Marov M. Ya. (1972) Venus: a perspective at the beginning of planetary exploration. *Icarus* **16**, 415–461.

Mills F. P. (1998) I. Observations and photochemical modeling of the Venus middle atmosphere. II. Thermal infrared spectroscopy of Europa and Callisto. Doctoral Thesis, California Institute of Technology, Pasadena, CA.

Morgan J. W. and Anders E. (1980) Chemical composition of the Earth, Venus, and Mercury. *Proc. Natl. Acad. Sci.* **77**, 6973–6977.

Mueller R. F. (1963) Chemistry and petrology of Venus: preliminary deductions. *Science* **141**, 1046–1047.

Nagy A. F. and Cravens T. E. (1997) Ionosphere: energetics. In *Venus II* (eds. S. W. Bougher, D. M. Hunten, and R. J. Phillips). University of Arizona Press, Tucson, pp. 189–223.

Pettengill G. H. (1968) Radar studies of the planets. In *Radar Astronomy* (ed. J. V. Evans). McGraw-Hill, NY, pp. 275–321.

Pettengill G. H., Ford P. G., and Simpson R. A. (1996) Electrical properties of the Venus surface from bistatic radar observations. *Science* **272**, 1628–1631.

Pettengill G. H., Campbell B. A., Campbell D. B., and Simpson R. A. (1997) Surface scattering and dielectrical properties. In *Venus II* (eds. S. W. Bougher, D. M. Hunten, and R. J. Phillips). University of Arizona Press, Tucson, pp. 527–546.

Pieters C. M., Head J. W., Patterson W., Pratt S., Garvin J., Barsukov V. L., Basilevsky A. T., Khodakovsky I. L., Selivanov A. S., Panfilov A. S., Gektin Yu. M., and Narayeva Y. M. (1986) The color of the surface of Venus. *Science* **234**, 1379–1383.

Schaber G. G., Strom R. G., Moore H. J., Soderblom L. A., Kirk R. L., Chadwick D. J., Davson D. D., Gaddis L. R., Boyce J. M., and Russell J. (1992) Geology and distribution of impact craters on Venus: what are they telling us? *J. Geophys. Res.* **97**, 13257–13301.

Seiff A. (1983) Thermal structure of the atmosphere of Venus. In *Venus* (eds. D. M. Hunten, L. Colin, T. M. Donahue, and V. I. Moroz). University of Arizona Press, Tucson, pp. 215–279.

Shapiro I. I. (1968) Spin and orbital motions of planets. In *Radar Astronomy* (ed. J. V. Evans). McGraw-Hill, NY, pp. 143–185.

Shapiro I. I., Campbell D. B., and DeCampli W. M. (1979) Nonresonance rotation of Venus? *Astrophys. J.* **230**, L123–L126.

Solomon S. C., Bullock M. A., and Grinspoon D. H. (1999) Climate change as a regulator of tectonics on Venus. *Science* **286**, 87–90.

Surkov Yu. A., Barsukov V. L., Moskalyeva L. P., Kharyukova V. P., and Kemurdzhian A. L. (1984) New data on the composition, structure, and properties of Venus rock obtained by Venera-13 and Venera-14. *J. Geophys. Res.: Proc. 15th LPSC* **89**, 393–402.

Surkov Yu. A., Moskalyova L. P., Kharyukova V. P., Dudin A. D., Smirnov G. G., and Zaitseva S. Ye. (1986) Venus rock composition at the Vega-2 landing site. *J. Geophys. Res. Proc. 17th LPSC* **91**, 215–218.

Surkov Yu. A., Kirnozov F. F., Glazov V. N., Dunchenko A. G., Tatsy L. P., and Sobornov O. P. (1987) Uranium, thorium, and potassium in the Venusian rocks at the landing sites of Vega-1 and Vega-2. *J. Geophys. Res.: Proc. 17th LPSC* **92**, 537–540.

Symonds R. B., Rose W. I., Bouth G. J. S., and Gerlach T. M. (1994) Volcanic-gas studies: methods, results, and applications. In *Volatiles in Magmas* (eds. M. R. Carroll and J. R. Holloway). Mineralogical Society of America, Washington, DC, pp. 1–66.

Tanaka K. L., Senske D. A., Price M., and Kirk R. L. (1997) Physiography, geomorphic/geologic mapping, and stratigraphy of Venus. In *Venus II* (eds. S. W. Bougher, D. M. Hunten, and R. J. Phillips). University of Arizona Press, Tucson, pp. 667–694.

Volkov V. P. and Frenkel M. Ya. (1993) The modeling of Venus' degassing in terms of potassium–argon system. *Earth Moon Planet.* **62**, 117–129.

Volkov V. P., Zolotov M. Yu., and Khodakovsky I. L. (1986) Lithospheric-atmospheric interaction on Venus. In *Chemistry and Physics of Terrestrial Planets* (ed. S. K. Saxena). Springer, New York, pp. 136–190.

Von Zahn U., Kumar S., Niemann H., and Prinn R. (1983) Composition of the Venus atmosphere. In *Venus* (eds. D. M. Hunten, L. Colin, T. M. Donahue, and V. I. Moroz). University of Arizona Press, Tucson, pp. 299–430.

Warneck P. (1988) *Chemistry of the Natural Atmosphere*. Academic Press, San Diego.

Wieler R. (2002) Noble gases in the solar system. In *Noble Gases in Geochemistry and Cosmochemistry* (eds. D. Porcelli, C. J. Ballentine, and R. Wieler). *Rev. Mineral. Geochem.* **47**, 21–70.

Wilson M. (1989) *Igneous Petrogenesis*. Unwin Hyman, London.

Woolf H. (1959) *The Transits of Venus a Study of Eighteenth-Century Science*. Princeton University Press, Princeton, 258pp.

Yung Y. L. and DeMore W. B. (1982) Photochemistry of the stratosphere of Venus: implications for atmospheric evolution. *Icarus* **51**, 199–247.

Treatise on Geochemistry
ISBN (set): 0-08-043751-6
Volume 1; (ISBN: 0-08-044336-2); pp. 487–507

Chile â€¡Department of Physics and McDonnell Center for the Space Sciences, Washington University, St. Louis, MO 63130, USA Â§ Centre for Cosmology, Particle Physics and Phenomenology, UniversitÂ´e. catholique de Louvain, Louvain-la-Neuve B-1348, Belgium Â¶Instituto de FÂ´Ä±sica, Universidade de SËœao Paulo, C. P. 66.318, 05315-970 SËœao. Paulo, Brazil Physik Department T70, Technische UniversitÂ¨at MuÂ¨nchen, James Franck StraÃŸe. Find everything you need to know about Washington University in St. Louis, including tuition & financial aid, student life, application info, academics & more.Â Campus Box 1089, 1 Brookings Drive, St. Louis, MO 63130 | (314) 935-5000. St. Louis, MO | (314) 935-5000. #19 in National Universities. 2020 Quick Stats.